MICROCOPY RESOLUTION TEST CHART

NATIONAL BUREAU OF STANDARDS-1963-A

AD-A164 079

UNCLASSIFIED

REPORT DOCUMENTATION PAGE	READ INSTRUCTIONS BEFORE COMPLETING FORM	
1. REPORT NUMBER ARO 16755.9-GS	2. GOVT ACCESSION NO. N/A	3. RECIPIENT'S CATALOG NUMBER N/A

TITLE (and Subtitle) Radiation Climate and Turbulence Structure of a Tropical Dry Evergreen Forest	5. TYPE OF REPORT & PERIOD COVERED Final, 10/25/79-6/15/85
	6. PERFORMING ORG. REPORT NUMBER

7. AUTHOR(s) R.T.Pinker	8. CONTRACT OR GRANT NUMBER(s) DAAG29-80-C-0012

9. PERFORMING ORGANIZATION NAME AND ADDRESS Department of Meteorology University of Maryland College Park,MD 20742	10. PROGRAM ELEMENT, PROJECT, TASK AREA & WORK UNIT NUMBERS

11. CONTROLLING OFFICE NAME AND ADDRESS U. S. Army Research Office Post Office Box 12211 Research Triangle Park, NC 27709	12. REPORT DATE November 1985
	13. NUMBER OF PAGES 121

14. MONITORING AGENCY NAME & ADDRESS(if different from Controlling Office)	15. SECURITY CLASS. (of this report) Unclassified
	15a. DECLASSIFICATION/DOWNGRADING SCHEDULE

16. DISTRIBUTION STATEMENT (of this Report)

Approved for public release; distribution unlimited.

17. DISTRIBUTION STATEMENT (of the abstract entered in Block 20, if different from Report)

NA

18. SUPPLEMENTARY NOTES

The view, opinions, and/or findings contained in this report are
those of the author(s) and should not be construed as an official
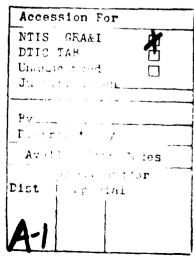Department of the Army position, policy, or decision, unless so
designated by other documentation.

19. KEY WORDS (Continue on reverse side if necessary and identify by block number)

Tropical Forest; Turbulence; Radiation Climate;Dispersion parameters;
Wind Structure in Forests;Rough Terrain.

20. ABSTRACT (Continue on reverse side if necessary and identify by block number)

DTIC FILE COPY

ABSTRACT

The research under this grant was based on information collected during the TREND (Tropical Environmental Data) experiment conducted during 1967-70 in a tropical forest environment in Southeast Asia. Under this grant we completed the data reduction process and conducted numerous scientific investigations which dealt with such topics as: radiation climate of the tropical forest; radiative transfer in vegetative canopies; seasonal variation in the radiation balance at canopy/air, ground/air interface; seasonal turbidity characteristics over the tropical forest; the temporal variation and stability dependence of the turbulence structure above and below the canopy; wind direction shear in the dense, semi-flexible tall vegetation; and variability parameters within and above the canopy, which characterize the dispersion process under different stability and ambient wind conditions.

Accession For	
NTIS GRA&I	☒
DTIC TAB	☐
Unannounced	☐
Justification	
By	
Distribution /	
Availability Codes	
	Avail and/or
Dist	Special

A-1

Radiation Climate
and
Turbulence Structure
of a
Tropical Dry Evergreen Forest

Final Report

Submitted to:
The Army Research Office
Durham, North Carolina

Grant No. DAA G29-80-C-0012

September 1985

Prepared by:
R. T. Pinker

Department of Meteorology
University of Maryland
College Park, MD 20742

SR-85-29

Radiation Climate
and
Turbulence Structure
of a
Tropical Dry Evergreen Forest

Final Report

Submitted to:
The Army Research Office
Durham, North Carolina

Grant No. DAA G29-80-C-0012

September 1985

Prepared by:
R. T. Pinker

Department of Meteorology
University of Maryland
College Park, MD 20742

SR-85-29

TABLE OF CONTENTS

LIST OF TABLES

12.   An example of the turbulence statistics output for each hourly data set. For each measurement level the following is given: the number of observations in each hourly sample; average values of $\bar{T}$, $\bar{V}$, $\bar{u}$, $\bar{\theta}$ and their standard deviations (σ_T, σ_V, σ_u, σ_v, σ_θ) from the hourly mean; the covariances ($\overline{u'T'}$, $\overline{v'T'}$, $\overline{u'v'}$, $\overline{V'T'}$, $\overline{\theta'T'}$).

13.   Histograms of the frequency distributions of temperature, wind direction and the u and v components for June 24, 1970, 21:30 p.m. (Such histograms were computed for each hourly sample).

14.   Key to stability parameters.

15.   Average observed Ri number (June data only) at each Pasquill class and model derived Ri numbers, using the formulation of Businger (1973) for the nondimensional temperature and wind profiles. Two values for the roughness parameter z_0, over the forest were assumed.

16.   Range of values for the Ri number upper limit for the Pasquill classes as derived by Sedefian and Bennet (1980), using several formulations of the nondimensional temperature and wind profiles. A roughness parameter $z_0 = 3$ cm was assumed.

17.   Frequency distributions of the number of cases in each Pasquill class and in a certain interval of Ri numbers (A), serving as a basis for establishing the upper and lower limits on the Ri number for each Pasquill class (B).

18.   Comparison of σ_θ's over the forest and clearing with those obtained by other investigators for the Pasquill classes (S-V: Sadhuran and Vittal Murthy (1983); P-G: Padmanabha Murthy (1979); Slade (1968); S: Shirvaikar (1975).

19.   A summary of turbulence statistics over the clearing and forest, as a function of the Pasquill classes for: a) February; b) April-May; c) June and d) August, 1970.

20.   Mean hourly wind direction shear and its standard deviation in the specified layers of the forest and clearing for the seven June days. N - neutral; U - unstable; S - stable; D - day; N - night.

LIST OF FIGURES

Figure

14. A normalized average (over day and season) wind profile on a log-log scale (x), and the predicted profile (Δ), and the scatter around the predicted mean obtained with $"a"_u$, $"a"_l$, and $"a"_u \pm \sigma_u$, $"a"_l \pm \sigma_l (\nabla)$, (   ), as given in Table 8.

15. a) An exponential least-square fit ($R_c = ae^{h/H} + b$) to the mean coupling rations (R_c) as a function of the normalized canopy depth (h/H) for h/H<1. Curve A: Using two-week averaged half-hourly data from all seasons stratified by wind speed at the 46 m level. Curve B: Using two-week averaged half-hourly data, stratified by month. Lower abscissa scale should be used with Curve B.

   b) Same as (a), with additional stratification by day (8 a.m. - 6 p.m.) and night.

16. The diurnal variation of the lapse rate (γ) in the 32-46 m layer above the forest and the 1-16 m layer above the clearing; the diurnal variation of the temperature (T) at the 1 m level in the clearing, 30 m level in the forest and the wind speed (W.S.) at the 46 m level in the clearing:

   a) for June 20, 1970; b) for June 25, 1985; d) for June 26, 1970; e) for June 27, 1970; f) for June 28, 1970.

17. a) The diurnal variation of the wind speed standard derivation (σ_V) for all eight (FT) levels, for June 23, 1970.

   b) Same as Fig. 3a for the (CT).

18. a) The diurnal variation of the wind direction standard deviation (σ_θ) for all eight (FT) levels for June 23, 1970.

   b) Same as Fig. 18a for the (CT).

19. Mean hourly standard deviation of 10-sec wind speed (abscissa) vs. height. a) clearing tower; b) forest tower.

20. Scattergrams of hourly standard deviations of 10-sec wind speed vs hourly mean wind speed for different stability classes and at different levels along the forest (FT) and clearing (CT) towers. Results are illustrated for the following cases: a) FT, 36 m, neutral; b) FT, 32 m, neutral; c) FT, 30 m, neutral; d) CT, 3 m, neutral.

21. Hourly standard deviation of 10-sec wind speed vs hourly mean wind speed. Linear regression curves for four stability categories. a) clearing tower, 16 m; b) forest tower, 36 m.

22. Same as Fig. 19 with slope of linear regression of σ_v vs $\overline{v}$ as abscissa.

23. Same as Fig. 19 with intercept of linear regression of σ_v vs $\bar{V}$ as abscissa.

24. Same as Fig. 19 with average intensity of turbulence $\sigma_v/\bar{V}$.

25. Same as Fig. 24, normalized by u_*.

26. Same as Fig. 25 for σ_{aw} and σ_{cw}.

27. Intensities of turbulence versus $(z-d)/z_o$. Symbols:
     $\triangle$ - Kansas (18 cm wheat stubble);
     O - Hiratsuka (open ocean);
     $\triangle$ - Tamano (20 cm rice stubble);
     X - Hamamatsu (flat soil surface);
     O - Kurashiki -1 (60 cm paddy field);
     O - Kurashiki -2 (90 cm paddy field);
     C - Forest clearing in Thailand;
     f - Tropical forest Thailand (32 m; z_o = 170 cm);
     f' - Tropical forest Thailand (32 m; z_o = 45 cm);
     a) $\sigma_u/\bar{V}$; b) $\sigma_v/\bar{V}$; c) $\sigma_w/\bar{V}$

28. The June (seven day), 1970 average wind profile along the forest and clearing towers. The average wind speed at the 46 m level of the FT approximates the wind speed at the 24 m level of the CT.

29. The distribution of the stability according to independently derived Ri numbers and Pasquill classes for a sample covering February June and August, 1970.

ABSTRACT

This report summarizes work done under Grant DAAG29-80-C-
0012 entitled: "Radiation Climate and Turbulence Structure of a
Tropical Dry Evergreen Forest", from the U. S. Army Research
Office, Durham, N.C., to the University of Maryland.

The research under this grant was based on information
collected during the TREND (Tropical Environmental Data)
experiment conducted during 1967-70 in a tropical forest
environment in Southeast Asia. Under this grant we completed the
data reduction process and conducted numerous scientific
investigations which dealt with such topics as: radiation
climate of the tropical forest; radiative transfer in vegetative
canopies; seasonal variation in the radiation balance at
canopy/air, ground/air interface; seasonal turbidity
characteristics over the tropical forest; the temporal variation
and stability dependence of the turbulence structure above and
below the canopy; wind direction shear in the dense, semi-
flexible tall vegetation; and variability parameters within and
above the canopy, which characterize the dispersion process under
different stability and ambient wind conditions.

In this report only selected results will be presented. A
detailed list of references to publications resulting from this
project can be found in Appendix A. Information about the final
data products resulting from this project can be found in
Appendix B.

BACKGROUND

A unique set of micrometeorological data was obtained during a multi-disciplinary environmental field program called Project TREND (Tropical Environmental Data) under the management of the Earth Sciences Laboratory, U. S. Army Natick Laboratories, Natick, Massachusetts and carried out by the Applied Scientific Research Corporation of Thailand (ASRCT) in collaboration with several Thai governmental agencies.

The experimental site was a tropical dry evergreen forest of about 80 square kilometers, situated at 14°31'N, 101°55'E in Thailand at elevations between 300 and 600 m (Fig. 1). The region is under the monsoonal regime of southeast Asia with two distinct seasonal circulations: a dry winter outflow from a cold continental anti-cyclone, and a moist summer inflow into a continental heat low. The climate is classified as tropical Savannah with annual rainfall of 1500 mm. A more detailed description of the site, climate, and microclimate can be found in Thompson and Landsberg (1975), Thompson and Pinker (1975), Pinker (1980) and Pinker et al. (1980).

The experimental design for the micrometeorological survey called for the collection and processing of: temperature, dew point temperature, wind speed and direction at numerous levels along two 46 meter towers (one in the forest and the other in a nearby clearing); radiation fluxes near the ground of both towers and at the top of the forest tower; and, precipitation above and below the canopy. Additionally, data on temperature, relative humidity, precipitation, evaporation and hours of

Figure 1. The experiment site with location of towers.

sunshine, at various ground stations in the experimental area, were collected. In Fig. 2, the schematic representation of the sensor levels along the towers is illustrated. The various tower data were sampled about once per ten seconds for a period of almost one year (Pinker and Kaylor, 1983a; 1983b). The data were stored on magnetic tapes using a sophisticated automatic data acquisition system (HP Model 7259), used in an analog and digital mode. A general account of the instrumentation and monitoring procedures is given in ASRCT (1969) and Dalrymple (1975). The key climatological parameters of the experimental area are summarized in Figs. 3, 4.

This project was a direct outgrowth of two previous contracts between the University of Maryland and:

1) The U. S. Army Topographic Engineer Laboratory Fort Belvoir, Virginia, U.S.A., Grant DAAK02-72-C-0287;

2) U. S. Army Research Office, Research Triangle Park, North Carolina, Grant DRXRO-GS-13660.

Under these grants the University of Maryland developed data processing procedures for extracting data from the original tapes and repacked these data in a format convenient for high speed computer analysis. Research related to the micrometeorological and microclimatological characteristics of the tropical evergreen forest was also conducted (Appendix A).

Under the present grant, the data reduction process was completed. All the tapes were repacked at high density of 6250 bpi (capability which did not exist at the University of Maryland

TEMPERATURE: ALL LEVELS

DEW POINT: ALL LEVELS EXCEPT 16

WIND SPEED, DIRECTION: LEVELS WITH SOLID LINES

PRECIPITATION: LEVELS 1, 16

SUBSURFACE TEMPERATURE: 5, 10, 20, 50, 100 cm

FOREST   CLEARING

Figure 2.   The position of the measurement levels along the towers.

6

Figure 4. Annual variation of climatological conditions at the experimental site for 11 - 1967 to 9 - 1970.

Figure 3. Wind-rose diagram for Nakhon Ratchasima situated 60 km North from experimental site for 1956-1960, from ASRCT (1967). The number in center represents percentage frequency of calms.

Computer Science Center before). The wind speed and wind direction data which were originally written on two separate tape systems with no correspondence between start and stop times were merged. Numerous invesigations were conducted and were oriented toward the characterization of the radiation climate and turbulence structure of the forest environment. The results obtained from our studies are a valuable source of information on the micrometeorology of tropical forests and are being utilized by numerous scientists.

Selected topics will be reviewed in two sections, one dealing with the radiation climate (I) and the other (II) with the turbulence structure of the tropical forest environment.

I. RADIATION CLIMATE

The radiation data acquired at the three platforms (top of forest tower; 1 m above the forest floor and, 1 m above the clearing ground) were sampled at a frequency of about 20 s. Half hourly averges were obtained and served as a basis for analyses.

The following variables were measured:

- global short wave and reflected short wave radiation - (miniaturized Eppley precision spectral pyranometer)

- standard WMO broad band spectral regions - (Eppley precision pyranometer with Schott filters - OG1 and OG2 broad band filters)

- total direct shortwave and spectral regions - (normal incidence Eppley pyrheliometers and Schott OG-1, RG-2, RG-8, GG-14 and WG-7 broad band filters)

- daylight illumination and UV - (Eppley photometers)

- incoming and outgoing total radiation (0.3-60 µm range) - (Funk radiometers).

- narrow band (100 nm) spectral regions - (by interference type filters)

All the available half hourly averaged repacked radiation data were inspected. The best data base was selected, edited and prepared for analysis (for details see Pinker and Kaylor, 1983b). Table 8 gives a detailed inventory of the radiation data that was edited.

1. THE RADIATION CLIMATE OF THE FOREST ENVIRONMENT

   a. Summary

   This study is based on measurements of:

   a) incoming and reflected global solar radiation (0.3 - 3 µm), as measured with Eppley precision pyranometers,

   b) incoming and outgoing total radiation (0.3 - 60 µm), as measured by a net pyrradiometer,

at the top and at the floor of the forest canopy. Before and after use, the precision pyranometers were calibrated by the Eppley company (accuracy of calibration was ±1%) while the Funk pyrradiometers were tested and calibrated by CSIRO, Aspendale, Australia (accuracy of calibration was ±2.5%). In what is to follow, a brief summary of radiation climate related topics will be presented.

b. Results

For all five periods of the year which were studied
(Table 1), the average daily total radiation received at forest
top (in the 0.3-60 µm range) is in excess of 1200 ly (50 MJ/m^2).
The average daily total received at forest floor (in the 0.3-60 µm
range) is about 920 ly (38.5 MJ/m^2), i.e., it amounts to 3/4 of
the daily total at the canopy top. The average daytime total
received at the forest top is about 800 ly (33.5 MJ/m^2) so that
the daytime contribution to the daily downward total radiation is
about 65% while at the forest floor it is only 48%. The daily
total net radiation at forest top amounts to about 265 ly
(11 MJ/m^2) averaged over the year. At the forest floor, there is
a net loss of 23 ly (0.96 MJ/m^2) in February. During the
remaining seasons that were studied, the daily total net

Month	level	daily total down(24 hrs) (.3-60µm) ly	max value down (.3-60µm) ly/min	daytime total down($\sim$11 hrs) (.3-60µm) ly	daily total net(24 hrs) (.3-60µm) ly	average mid-day albedo
Feb.	FT	1250.2	1.8	849.4	276.1	12.5
	FF	903.5	.67	421.4	-23.5	
March	FT	1213.1	1.7	826.9	228.6	10.8
	FF	949.7	.82	460.1	18.6	
June	FT	1252.7	1.6	797.0	282.7	11.5
	FF	942.4	.78	454.0	26.6	
Aug.	FT	1201.6	1.7	750.4	258.6	11.9
	FF	907.6	.70	430.7	14.3	
Sept.	FT	1230.5	1.7	788.6	279.5	11.7
	FF	915.1	.77	437.8	19.9	
Average	FT	1229.6	1.5	802.5	265.1	11.7
	FF	923.7	.75	440.8	13.4	

Table 1. Average radiation balance information (.3-60 um range)
above the forest top (FT) and at the forest floor
(FF).

radiation at forest floor was positive and the overall average value was about 13 ly ($0.54\,MJ/m^2$). Thus, averaged over the year, the net radiation near the ground within the forest amounted to about 5% of that at the forest top.

As evident from Table 2, the average daily total (~11 hrs) of shortwave radiation (0.3-3 µm) at forest top is about 420 ly and at forest floor only 34 ly (i.e., it amounts only to 8.2% of the corresponding value at forest top). The daily total (24 hrs) of the downward longwave (3-60 um) radiation at the forest floor is about 8.3% higher than the corresponding value at the forest top. The average longwave radiation at the forest top is at the rate of 0.56 ly/min and at the forest floor at the rate of 0.61 ly/min. Regression equations between the shortwave and net

Month	# of days	level	24 hr total down (.3-60 µm) ly	daytime total down (11 hrs) (.3-3 µm) ly	24 hr total down (3-60 µm) ly	daytime total down (11 hrs) (.3-60 µm) ly	daytime total down (11 hrs) (3-60 µm) ly	24 hour average down (3-60 um) ly/min
Feb.	7	FT	1283.5	507.0	776.5	886.8	379.8	.53
		FF	904.8	37.2	867.6	424.1	386.9	.60
March	11	FT	1207.0	422.7	784.3	815.6	393.0	.54
		FF	946.3	42.7	903.6	456.5	413.9	.62
June	11	FT	1270.1	412.7	857.4	855.8	443.0	.59
		FF	929.2	30.5	898.7	484.2	453.7	.62
Aug.	10	FT	1201.6	360.3	841.4	787.7	427.4	.58
		FF	907.6	22.7	884.5	467.5	444.8	.61
Sept.	11	FT	1235.4	404.4	831.0	829.0	424.6	.57
		FF	916.2	39.1	877.1	475.0	435.9	.60
verage		FT	1239.5	421.4	818.1	835.0	413.6	.56
		FF	920.8	34.4	886.3	461.5	427.0	.61

Table 2. Average shortwave (SW) (.3-3 um) and longwave (LW) (3-60 um) radiation balance information above the forest top (FT) and at the forest floor (FF).

radiation were developed for each month (Table 3). The highest
correlations were found during clear periods (Pinker et al. 1980).
More details can be found in Pinker, et al. (1980).

month	# of days	regr coeff b	intercept a(mly/min)	intercept a(w/m^2)	error in b	error in a mly/min	error in a (w/m^2)	% of variance explained	correl	mean mly/min R_n	R_{sw}
Feb.	7	.93	-116.91	-81.6	.01	4.55	3.0	99.523	.9976	599.3	768.2
March	11	.88	-60.55	-42.0	.01	4.50	3.0	98.881	.9944	501.8	640.4
June	11	.87	-21.46	-15.0	.01	8.96	6.0	94.352	.9714	475.3	573.3
Aug.	10	.86	-31.86	-22.0	0.00	2.39	2.0	99.565	.9978	400.7	500.3
Sept.	11	.87	-41.02	-28.0	0.00	2.60	2.0	99.518	.9976	446.3	561.7

Table 3. Information about the regression relationship between
the shortwave radiation (R_{sw}) and the net
radiation (R_n) at canopy level.

The flux density distribution of solar radiation in
vegetative canopies is generally not normal. This implies that
use of a single value predictors (e.g., the mean) for calculating
the rates of processes varying nonlinearly with radiant flux
density (i.e., photosynthesis) leads to error. In Fig. 5, the
frequency distributions of the various flux densities below and
above the canopy are presented and the relevant statistics of
these distributions are summarized in Table 4.

Period	#days	Mean FT	FF	St. Dev. FT	FF	Skew FT	FF	Kurt FT	FF	Normality at 95% cont. lev. FT	FF
Feb	8	624.8 (34.6)	50.3 (5.9)	458.5 (24.4)	78.3 (4.2)	.19 (.19)	4.21 (.19)	-1.46 (.37)	20.3 (.37)	rej	rej
March	13	630.3 (23.0)	61.7 (4.5)	388.2 (16.2)	75.9 (3.2)	.24 (.15)	2.56 (.15)	-1.16 (.29)	6.97 (.29)	rej	rej
June	12	582.5 (22.5)	42.9 (2.9)	382.4 (15.9)	49.3 (2.1)	.40 (.14)	3.65 (.14)	-.91 (.29)	19.0 (.29)	rej	rej
Aug	10	500.3 (26.3)	31.5 (1.5)	406.9 (18.6)	73.6 (1.1)	.73 (.16)	1.29 (.16)	-.49 (.32)	2.38 (.32)	rej	rej
Sept	12	575.8 (24.6)	54.8 (4.9)	417.8 (17.4)	83.0 (3.5)	.40 (.14)	4.52 (.14)	-.97 (.29)	25.09 (.29)	rej	rej

Table 4. Pertinent statistics on the frequency distributions of the global solar radiation flux, above and below the forest canopy during several months of 1970.

2. THE SURFACE ALBEDO

a. Summary

The diurnal variation of the average albedo over the tropical forest and a nearby clearing were investigated. The average mid-day albedo for the winter monsoon season was established to be 10.6% for the forest and 13.4% for the clearing. During the summer monsoon, it was 12.0% and 14.6% respectively. The amplitude of the diurnal variation was substantially reduced during the cloudy conditions but the mid-day albedo was higher than the clear sky mid-day albedo. Asymmetry around solar noon in the albedo was found during both clear and cloudy conditions.

b. Background

In studies related to the energy balance at the ground/air

interface it is common to use the mid-day albedo value as representative of the daily average. This can lead to an error in estimating the net radiation. This study examined the diurnal variation and the asymmetry around solar noon in the forest and clearing albedos. The results reported here are based on half-hourly averages of the global shortwave and reflected shortwave radiation (0.3-3 μm) measured with the Eppley precision pyranometers.

c. Results

The average noontime (10 a.m. - 2 p.m.) albedo for the winter monsoon season was found to be 10.6% for the forest and 13.4% for the clearing. During the summer monsoon it was 12.0% for the forest and 14.6% for the clearing. The diurnal variation of the average albedo is illustrated in Fig. 6 for two characteristic periods. In March, clear sky conditions dominate (18 days with >8 hrs of sunshine) while August is cloudy (4 days with >8 hrs of sunshine). The noon albedo in March is about 10.8%, while in August, it approaches 12%. This is at odds with findings over conifer forests in temperate climates where no significant differences between clear and cloudy conditions were found (i.e., Stewart, 1971).

In the progress of this investigation, it became apparent that an asymmetry around solar noon in the albedo values existed. Three cases are presented (Figs. 7, 8), where the albedos are plotted as a function of the sun's elevation. Two of the cases illustrate clear sky conditions, while one depicts cloudy conditions. The asymmetry in the albedo around solar noon

is common to all three cases. This would exclude the specular reflectivity of the direct beam component due to differences in leaf orientation, as a plausible cause of the asymmetry. During the cloudy and wet August, the asymmetry is present even though the diurnal variation characteristic of the clear cases is suppressed. The above noted differences and similarities in the asymmetry pattern suggest that the variation in vegetation moisture is a possible cause. For details see Pinker et al. (1980) and Pinker (1980).

3. THE ULTRA-VIOLET RADIATION OF THE FOREST ENVIRONMENT

   a. Summary

A unique set of UV and shortwave radiation data, collected in the tropical forest environment was analyzed. It was found that only about 10% of the ambient UV radiation will reach the forest floor and that this latter constitutes 2-5% of the total Global Short Wave radiation (UV/GSW) at the ground. A similar ratio of 2-5% was found for UV/GSW above the canopy.

   b. Background

UV radiation is known to have beneficial effects, such as the synthesis of Vitamin D in the superficial layers of skin, and harmful effects, such as the induction of skin cancer and aggravation of drug-induced light-sensitivity of the skin. It is also known to affect mutations, color changes in fungi, and degradation of materials. In spite of the considerable interest

Figure 5. Frequency distributions of global solar radiation intensities (a) above and (b) below the forest canopy for: February; March; June; August and, September, 1970.

Figure 5. Continued

Figure 5. Continued.

Figure 5. Continued.

Figure 5. Continued.

Figure 6. The diurnal variation of the albedo for an average
day in: (a) March, 1970; (b) August, 1970.

Figure 7. The albedo of the forest and clearing for: a) a
clear day in February (10.2 hours of sunshine out of
11.1 hours possible), b) a clear day in March (9.1
hours of sunshine out of 12.1 hours possible), as a
function of solar elevation.

21

that many disciplines have in UV radiation, relatively little is known on how much of it is received at the earth's surface. At the TREND site, the UV radiation was measured with an Eppley Photometer utilizing Weston Selenium barrier layer photocells. It had a sealed-in quartz window, a band-pass filter that restricted the wavelength response of the photocell to the desired range (0.29 - 0.38 µm) and a diffusing disk of opaque quartz. The results reported here are based on half-hourly averages of the UV radiation (0.29-0.38 µ,m) and corresponding half-hourly averages of the global shortwave radiation (0.3 - 3.0 µm).

c. Results

The average daily totals of the UV radiation above and below

PERIOD (1970)	# OF DAYS	DAILY TOTAL UV(FT)(ly)	DAILY TOTAL UV(FF)(ly)	UV(FT)/GSW(FT) (%)	UV(FF)/GSW(FF) (%)
Feb	11	21.1	1.8	3.2	3.8
Mar	13	17.8	1.6	2.7	2.6
May	11	19.9	4.0	3.1	9.7
Jun	12	15.2	1.7	2.7	4.0
Aug	17	18.0	1.4	3.8	3.3
Sep	12	18.2	1.6	3.2	2.9

Table 5. Information about the average daily total UV radiation at the forest site. Measurements were taken at the forest top (FT) and forest floor (FF). Ratios of UV radiation to total global shortwave (GSW) radiation are also presented.

the forest canopy are presented in Table 5. Approximately, 10%
of the UV radiation above the canopy reaches the ground. Similar
estimates of UV absorption by vegetation were reported by Gates
(1965) for single leaves. The values measured above the canopy
were in the range of 2-5% as also reported previously (Koller,
1952). It is of interest to note that the ratios below the
canopy are also within the range of 2-5%.

The diurnal variation in the intensity of the average UV
radiation and the average global shortwave radiation, above and
below the forest canopy, are illustrated for March and August
1970 in Fig. 9. Generally, the UV below the canopy follows the
UV above it, and both follow the variation in the global
shortwave radiation. More details can be found in Pinker (1984).

Figure 9. The diurnal variation of the average UV and shortwave radiation (.3-3 μm) above and below a tropical forest canopy for: a) March, 1970; b) August, 1970.

4. THE TURBIDITY OF THE FOREST SITE

a. Summary

In this study, a methodology was developed to analyze the broad-band Normal Incidence Pyrheliometer (NIP) spectral data collected with the Schott OG1, RG8 and WG7 filters for the purpose of estimating the turbidity conditions of the region. For the days sampled, it was found that the general Linke turbidity factor T_G, ranges from a minimum of 3.05 to a maximum of 7.15. Angstrom's turbidity parameters were also computed from the spectral pyrheliometer measurements, however, the accuracy of the data was evidently not sufficient to yield acceptable results.

b. Background

The measurement of the spectral direct beam solar radiation under cloudless sky conditions with proper correction for molecular scattering and absorption, enables a determination of atmospheric turbidity, defined as the extinction of solar radiation by suspended particles that are large with respect to the wavelength of light (radius range of about 0.1-10 um).

The amount of energy which reaches a pyrheliometer measuring the direct solar radiation at a given time is given by Beer's law as:

$$F = (1/S) \int_O^\infty F_O(\lambda)e^{-\tau(\lambda)m}d\lambda \tag{1}$$

$F_O(\lambda)$ is the spectral flux of solar radiation at the top of the atmosphere, m is the relative optical air mass, and S is the

Earth-Sun distance factor. The exponential factor $\tau(\lambda)$ is the total optical depth which is composed of individual optical depth due to Rayleigh scattering $\tau_R(\lambda)$, water vapor absorption $\tau_W(\lambda)$, ozone absorption (τ_{O3}), and aerosol extinction $\tau_A(\lambda)$. Linke's turbidity factor is defined by the equation

$$F = (1/S)\ F_O e^{-[T\ \bar{\tau}_R(m)m]} \tag{2}$$

where $\bar{\tau}_R(m)$ is the mean value of the Rayleigh optical depth weighted by the distribution of transmitted energy and integrated over all wavelengths. Specifically,

$$T = (\ln F_O - \ln F - \ln S)/(\bar{\tau}_R(m)m) \tag{3}$$

The scattering and absorption by solid and liquid particles can be described by Beer's law as

$$P_\lambda = e^{-f(\lambda)} \tag{4}$$

where the function $f(\lambda)$ depends on the wavelength and the qualities of the turbid medium producing the scattering and absorption.

Angstrom developed an empirical relationship for $f(\lambda)$ based on experimental data:

$$P_\lambda = e^{-\frac{\beta}{\lambda^\alpha}} \tag{5}$$

Equation (5) defines Angstrom's turbidity coefficient, β, and the wavelength exponent, α, which characterize the scattering and absorbing aerosol. From extensive observations in the atmosphere it was found that α varies from about 0.5 to 1.6. A value of α = 1.3 was found for many industrial regions. When the atmosphere is very polluted by large particles, (i.e., volcanic eruptions or forest fires) α may be reduced to a rather low value of 0.5 or less.

In order to compute the Angstrom turbidity coefficient β, Eq. (1) is expanded to show the components of the total optical depth:

$$F = (1/S) \int_0^\infty F_0(\lambda) \exp[-(\tau_R(\lambda) + \tau_{o3}(\lambda) + \tau_A(\lambda))m]d\lambda \qquad (6)$$

Substituting for τ_A from Eq. (5) for a single wavelength:

$$F(\lambda) = (1/S) F_0(\lambda) e^{-\tau_R(\lambda)m} e^{-\tau_{o3}(\lambda)m} e^{\frac{-\beta}{\lambda^\alpha}m} \qquad (7)$$

Solving Eq. (8) for β yields:

$$\beta = -\frac{\lambda^\alpha}{m} \ln \frac{}{F_0(\lambda)e^{-\tau_R(\lambda)m}} \qquad (8)$$

Angstrom's turbidity coefficient β can be calculated from Eq. (8) if an average value of α, is used and the Rayleigh and

ozone optical depths are calculated.

c. Procedures and Results

c.1 Linke's Turbidity Factors

Both Linke's general turbidity factor T_G and Linke's shortwave turbidity factor T_K (Kurzstrahlung) were computed from the broadband pyrheliometer measurements. The Manes and Joseph (1978) method for numerically determining atmospheric turbidity indices was used. Johnson's (1954) data for the extraterrestrial solar flux for 138 intervals in the wavelength range 0.22 μm to 7.0 μm were used. The wavelength corresponding to the center of each interval is related to the energy in each interval, as computed by trapezoidal integration. For each wavelength the Rayleigh scattering coefficients were computed by Allen's (1958) equation,

$$\tau_R(\lambda) = 1.025 \times 10^5 \, (n-1)^2 \lambda^{-4} \tag{13}$$

where λ - wavelength in microns, n - refractive index given as:

$$n-1 = A \, (1+B/\lambda^2), \quad A = 28.71 \times 10^{-5}, \quad B = 5.67 \times 10^{-3}.$$

For each broadband wavelength interval, the effective Rayleigh scattering optical depths averaged over a spectral range as a function of air mass were computed from

$$\bar{\tau}_R(m) = -\frac{1}{m}\frac{\int_{\lambda 1}^{\lambda 2} I_o(\lambda)e^{-\tau_R(\lambda)m}d\lambda}{\int_{\lambda 1}^{\lambda 2} I_o(\lambda)d\lambda} \qquad (14)$$

The optical airmass m is computed by

$$m = 1/\sin z \qquad (15)$$

where z - solar zenith angle.

Values of $\bar{\tau}_R(m)$ were calculated for a wide range of air masses in increments of 0.1. Linke's general and shortwave turbidity factors can then be computed using Eq. (3) with the calculated values of $\bar{\tau}_R(m)$ for 0-630 nm and for the total spectrum, and the measured values of the direct beam solar radiation in these two wavelength bands.

Figure 10 presents the frequency distribution of Linke's turbidity factors for the TREND site. Each value of T_G and T_K was computed for cases for which the optical airmass was less than 2.0. The exclusion of data with optical air masses greater than 2.0 was done to eliminate the effects of virtual variations due to variation of the optical air mass. For the days sampled, it is seen that the general turbidity factor, T_G, ranges from a minimum of 3.05 to a maximum of 7.15; the shortwave turbidity factor, T_K, ranges from a minimum of 1.03 to a maximum of 3.54.

c.2 Angstrom's turbidity factors

Angstrom's turbidity parameters were also computed from the spectral pyrheliometer measurements. Eq. (8) was used to

Figure 10. The frequency distribution of the Linke's turbidity factors, T_G (upper), and T_K (lower) for Thailand.

calculate the turbidity parameters β_g, β_{rg} and β_r for the three wavelength bands 0-525 nm, 525-630 nm, and 0-630 nm.

The calculation of Angstrom's turbidity parameters yielded unreasonable results. Mani et al. (1969) stated that a 1% error in the measurement of each of the broadband wavelength intervals can result in a 50% error in the determination of β_{rg} and a 100% error in the evaluation of α. Paltridge and Platt (1976) add that a 1% error in instrument calibration is equivalent to a 50% error in turbidity for low values of turbidity such as 0.02 which are not uncommon in clear atmospheres. Bahm and Nakos (1979) examined the calibration of pyrheliometers at several individual laboratories within the U.S. and found that presently, pyrheliometers have errors of about ±2%. More details can be found in Pinker and Eck (1981).

5. THE USE OF THE DELTA EDDINGTON APPROXIMATION FOR THE TRANSFER OF RADIATIVE ENERGY FLUXES THROUGH PLANT CANOPIES

   a. Summary

   During the TREND experiment a unique set of solar spectral data was collected above and below the forest canopy. To enable the interpretation of this information, an atmospheric radiative transfer model was adaped for use in vegetative canopies. The model was tested and proved to be useful with data from a corn canopy.

   b. Background

   The treatment of radiative transfer through vegetative

canopies has been attempted in the past by using probability methods, 2-stream approximation; Monte Carlo method; and Eddington approximation.

To calculate fluxes, the variants of two-stream and Eddington approximations are not sufficiently flexible to encompass the solar spectrum and the different vertical layers. In a canopy, one can encounter large variations in optical depth and single scattering albedo in the vertical. The existing approximations are valid for restricted ranges of these parameters and seem not to be able to handle the asymmetric phase functions typical of leaves. The delta-Eddington (d-E) approximation (Joseph et al. 1976) provides a method for rapid and accurate calculation of monochromatic fluxes in an absorbing/scattering atmosphere for all phase functions, optical depths, and single scattering albedo.

The (d-E) approximation consists of replacing the actual scattering phase function by a Dirac delta function forward scattering peak that contains a fraction "f" of the scattering and the ordinary Eddington phase function for the remaining portion of the scattering, i.e.,

$$P(\mu) = 2f\ (1-\mu) + (1-f)\ (1+3g'\mu)$$

If g is the asymmetry factor of the actual phase function then,

$$g' = (g-f)/(1-f)$$

By requiring that the second moment of P agree with the second moment of the Henyey-Greenstein phase function, it can be shown that

$$f = g^2$$

Substituting the expression for $P(\mu)$ in the transfer equation and making the Eddington approximation that the diffuse radiation can be expressed in the form

$$N = N_o + \mu N_1$$

leads to solutions that are equivalent to solutions from the Eddington approximations but expressed in terms of a transfer single scattering albedo ω' and optical thickness τ' given as:

$$\omega' = (1-f)\ \omega/(1-\omega f)$$

$$\tau' = (1-\omega f)\tau$$

This approach is appropriate for a plant canopy since the canopy behaves as any other multiple scattering media, such as clouds. Also, it is desirable to characterize the optical properties of the atmosphere and plant canopies by a minimum number of parameters. These parameters are functions of depth within the atmosphere and canopy and will vary with wavelength of incident radiation. The (d-E) analysis reduces to three the number of parameters required to describe penetration of solar irradiance through a canopy.

In our study tests were done with the (d-E) approximation with available input data for corn for 1 μm. Some results are presented in Figures 11, 12. However, the data from the forest site were collected in broad spectral bands with cut-off filters which were selected to be relevant for atmospheric observations

34

Figure 11. Relative irradiance of 1 μm radiation within 250 cm high corn canopy,
0000 measured in Ithaca, NY,
____ predicted with the Eddington approximation,
____ predicted with the delta-Eddington approximation.

Figure 12. Fraction of incident 1 um solar irradiances abscrbed per centimeter in corn canopy,
_____ as computed with the delta-Eddington approximation,
_____ as computed with the Eddington approximation.

rather than for vegetation. These data were found to be restricted in their value for use with this model.

II. WIND AND TURBULENCE

The wind speed and direction data used in this section were collected at eight levels along the two towers. The wind speed sensors were Climet three-up anemometers having a threshold velocity of 0.3 m s^{-1}. A totalizing signal was read every 10 s. The wind direction was detected by Climet wind direction transmitters and vanes. The wind direction was sampled about once every 30 s. The instruments were calibrated before and after the experiment at the National Bureau of Standards (NBS), Washington, D.C., in 1968 and 1970. The uncertainty of the wind speed measurements prior to the experiment was reported as follows:

Air Speed, m s^{-1}	>13.4	4.5	2.2	1	0.5
Uncertainty	0.4%	0.8%	1%	5%	14%

The calibration record of 8/22/70 after the experiment reports allowable error of 1%.

In the studies dealing with the turbulence structure, use was made of the temperature data as well. Temperature measurements at both towers were made with Hewlett-Packard quartz thermometers placed in Climet shielded motored aspirators. The scanning period of the data acquisition system was such that all

42 channels of temperature could be scanned to an accuracy of 0.1°C within three seconds. However, the sampling rate was set so that measurements were made every 10 seconds.

6. THE CANOPY FLOW INDEX

   a. Summary

   The canopy flow in the two story tropical forest was investigated using a large sample of wind profiles which span the whole monsoon cycle. The canopy flow index ("a") concept was adopted as a possible way to model the canopy flow. It was found suitable to use two indices. Due to the large number of profiles available, this study could address the issues of the dependence of "a" on the ambient wind speed. No dependence seemed evident if winds of 2 m/sec above the canopy were exceeded. However, dependence on wind directions seems to be a plausible reason for the large variability in the index as indicated by the increased standard deviation of "a" for periods of less steady ambient flow.

   b. Introduction

   The turbulence within a vegetative canopy is generated by the breakdown of the atmospheric flow into eddies (externally induced) and by eddies generated by the many inhomogeneous elements that comprise the canopy (internally induced).

   Most of the mathematical models of canopy flow are based on the assumption of steady state flow in a horizontally infinite canopy under neutral thermal stratification. The basic differential equation so derived is:

$$\partial/\partial z \ (K(z)+\nu) \ \frac{\partial U}{\partial z} = \frac{A(z) \ C_D U^2}{2} \qquad\qquad (1)$$

where:

$K(z)$ - eddy viscosity

ν - molecular viscosity

U - mean horizontal wind speed

C_D - the form drag coefficient

$A(Z)$ - the leaf and branch area per unit volume

The left term represents the divergence of the Reynolds stress and the right term is equal to the fluid drag. This equation can be solved by different numerical techniques (Tan and Ling, 1963; Inoue, 1963; Cionco, 1965; Cowan, 1968; Silbert, 1970; Shaw, 1977).

The present study utilizes the formulation of Cionco (1965) who derived the following canopy flow equation:

$$\frac{1}{h} \frac{\partial U}{\partial x} \ [\frac{\partial U}{h^2 \partial x} \ \frac{\partial(\ln l_c)}{\partial x} + \frac{\partial^2 U}{h^2 \partial x^2}] = \frac{S U^2}{l_c^2} \qquad\qquad (2)$$

where:

$x = z/h$

z = height above surface

h = canopy height

l_c = mixing length in canopy

$S = 1/2 \ C_D \ A(Z)$

Using the assumptions of an idealized canopy with a mixing length that is constant with height this equation can be solved yielding:

$$U(z) = U(h) \exp [-a (1 - z/h)] \qquad (3)$$

where:

a = extinction coefficient

$$(a/h)^3 = \frac{C_D A(Z)}{2 l_c^2}$$

i.e., the wind speed falls off exponentially with a depth scale proportional to $2^{1/3} l_c^{2/3} (C_D A(Z))^{-1/3}$, where $A(Z)$ and C_D, or their product, are assumed constant with height.

Wind speed data for January, February, April, June, July and September were used. Approximately ten days of observations were available for each month. Each day had 48 wind profiles averaged half hourly: each half hourly value was based on 180 ten second data points. The average wind speeds at about 20m above the forest canopy are presented in Table 6. Similar information obtained along a tower in a nearby clearing is also included, to illustrate the drag effect of the forest canopy on the ambient wind field.

Period (in 1970)	Level m	CT		FT	
		Vel. m/sec	v_1/v_2	Vel. m/sec	v_1/v_2
January	46 32	2.84 2.42	1.17	2.200 0.566	3.88
February	46 32	6.47 5.47	1.18	4.84 2.25	2.15
April	46 32	4.75 4.06	1.17	3.63 1.51	2.40
June	46 32	5.73 4.98	1.15	4.17 1.85	2.20
July	46 32	6.49 5.67	1.14	4.70 2.13	2.2
September	46 32	5.16 4.77	1.08	3.93 1.73	2.27

Table 6. Two-week averaged wind velocities at selected levels along the forest (FT) and clearing (CT) towers (V_1 - at the 46 m level, V_2 - at the 32 m level).

c. Procedures and results

For each period of study, the data were stratified according to wind speed at the highest measurement level above the canopy; the attenuation coefficient "a" was computed for each such group separately using Eq. (3). A least square fit was obtained for the computed "a" values. Table 7 presents summaries of all the results, i.e., average "a" for upper and lower canopy; correlation coefficients; intercepts and slopes. For all the months treated, there does not seem to be a dependence of "a" on ambient wind speed as long as winds of 2 m/sec are exceeded. The average values for all periods studied are summarized in Table 8. The range of the standard deviations during the various periods studied is indicated. The values of "a" as compiled by Cionco (1978) are summarized for comparison.

Table 7. Statistical summary about the computed canopy flow index "a".

Period	# of Cases	Wind speed range 20m above canopy (m/sec)	mean a 28-20m	mean a 12-4m	Standard Deviation 20-20m	Standard Deviation 12-4m	Correlation Coeff	regression Coeff	Intercept
January	0	> 5.0	--	--	--	--	--	--	--
	0	4.0 - 5.0	--	--	--	--	--	--	--
	30	3.0 - 4.0	--	--	--	--	--	--	--
	500	2.0 - 3.0	--	--	--	--	--	--	--
	500	0.0 - 2.0	--	--	--	--	--	--	--
February	468	> 5.0	4.00	2.03	0.63	0.40	.70	.09	1.54
	296	4.0 - 5.0	4.10	2.00	0.52	0.44	.74	.09	1.52
	188	3.0 - 4.0	3.99	1.67	0.47	0.30	.83	.11	1.03
	40	2.0 - 3.0	4.05	1.39	0.50	0.25	.88	.13	0.51
	8	0.0 - 2.0	3.64	1.29	0.67	0.31	.78	.10	0.42
April	52	> 5.0	4.63	1.81	1.39	0.25	.63	.12	1.27
	26	4.0 - 5.0	4.35	1.80	1.35	0.40	.63	.12	0.95
	51	3.0 - 4.0	4.21	1.64	2.51	0.70	.64	.16	0.52
	23	2.0 - 3.0	3.45	1.37	3.51	0.80	.54	.16	0.14
	20	0.0 - 2.0	2.74	1.13	3.27	0.63	.41	.10	-0.04
June	115	> 5.0	4.31	1.65	0.51	0.26	.82	.13	0.93
	82	4.0 - 5.0	4.25	1.82	0.60	0.33	.85	.13	1.03
	57	3.0 - 4.0	4.21	1.77	0.80	0.31	.86	.13	0.90
	17	2.0 - 3.0	4.03	1.63	0.98	0.25	.84	.13	0.59
	18	0.0 - 2.0	3.36	1.42	1.35	0.39	.26	.03	0.85
July	251	> 5.0	3.27	1.74	.73	.28	.85	.09	1.05
	190	4.0 - 5.0	3.38	1.85	.73	.30	.83	.09	1.21
	94	3.0 - 4.0	3.67	1.86	.85	.22	.80	.10	1.20
	16	2.0 - 3.0	3.80	1.88	.45	.23	.01	.09	1.34
	8	0.0 - 2.0	3.01	1.79	.85	.81	.06	.07	.06
September	142	> 5.0	2.69	1.66	1.32	.30	.84	.12	.64
	120	4.0 - 5.0	4.16	1.62	1.99	.40	.77	.16	.26
	184	3.0 - 4.0	4.45	1.67	2.20	.35	.78	.18	.12
	42	2.0 - 3.0	4.97	1.60	2.02	.32	.78	.22	-.31
	64	0.0 - 2.0	4.27	1.39	2.31	.33	.79	.18	-.29

Forest Canopy	"a" mean ± st. dev.
Gum - maple	4.42 ± 1.05
Maple - fir	4.03 ± 0.65
Jungle	3.84 ± 1.52
Spruce	2.74 ± 1.29
Oak - gum	2.68 ± 0.66
Tropical - evergreen	

	mean ± st. dev. range	
	upper canopy	lower canopy
> 5.0 *	$3.98 \pm (.25-1.32)$	$1.77 \pm (.25-.40)$
4.0 - 5.0	$4.05 \pm (.52-1.95)$	$1.81 \pm (.30-.44)$
3.0 - 4.0	$4.11 \pm (.47-3.51)$	$1.72 \pm (.30-.70)$
2.0 - 3.0	$4.06 \pm (.45-3.51)$	$1.57 \pm (.23-.80)$
0.0 - 2.0	$3.4 \pm (.67-3.25)$	$1.40 \pm (.31-.60)$

* wind speed range 20m above canopy

Table 8. Average canopy flow index "a" for forest canopies after Cionco (1978) and Shinn (1971) and for present study.

To test the suitability of the computed canopy flow index "a" to actual conditions, average profiles for each period investigated were compared to the model profile using the appropriate canopy index. The results are illustrated for selected cases in Figures 13 and 14. For more details see Pinker and Moses (1982).

7. THE CANOPY COUPLING INDEX

   a. Summary

It is common to characterize the canopy flow by what is known as a coupling index (R_c). In the present study, the dependence of the coupling index on ambient conditions and its variation with height inside the canopy were investigated.

42

CANOPY WIND PROFILES

Figure 14. A normalized average (over day and season) wind profile on a log-log scale (x), and the predicted profile (Δ), and the scatter around the predicted mean obtained with "a" $_u$, and "a" $_u \pm \sigma_u$, "a" $_l \pm \sigma_l (\nabla)$, ( ), as given in Table 8.

CANOPY WIND PROFILES

JULY

x – daily average
Δ – model

Figure 13. The normalized average wind profile on a log-log scale for July 1970 (x), and the predicted wind profile (Δ), using appropriate upper canopy "a" $_u$ and lower canopy "a" $_l$ values from Table 7.

Exponential functions which describe the height dependence of the coupling index were fitted to the various cases of data stratification; correlation coefficients as high as (.80) were obtained.

b. Background

The coupling index is defined as the ratio of the mean wind speed at certain reference level within the canopy and above it. It is a measure of the efficiency with which the momentum is transferred from the ambient wind field to the canopy.

The wind speed data used in this study were collected at eight levels along a 50 m high tower for December 1969, January, February, April, June, July and September of 1970. Two week averages of the 48 profiles were used to compute a representative coupling parameter at all the observational levels below the canopy.

c. Procedures and Results

c.1 Using measured wind profiles

The wind speed measurement levels selected for this study were those at the canopy top - 32 m (1H), at 46 m (1.44H) above ground, and at four levels inside the canopy; 30 m (0.9H), 25 m (0.78H), 16 m (0.50H) and 4 m (0.13H).

In order to assess the effect of the ambient wind speed on the coupling, all the data used were merged and stratified by the magnitude of the wind speed at the upper most observation level. The results are presented in Table 9. The mean values of the coupling index for each velocity interval at each measurement level were plotted in Figure 15(a); an exponential least square

fit to the coupling parameters is also illustrated.

Subsequently, the data were subdivided into daytime and

nighttime cases. The mean values of the coupling index for each

case at each measurement level are plotted in Fig. 15(b); an

exponential lease square fit to the coupling parameters is also

illustrated.

Wind Speed		U(1.00H)/U(1.44H)	U(0.94H)/U(1.44H)	U(0.78H)/U(1.44H)	U(0.50H)/U(1.44H)	U(0.13H)/U(1.44H)
V<2 m/sec	Mean	.263	.188	.138	.133	.138
	Std. Dev.	.030	.013	.004	.005	.002
2<V<3 m/sec	Mean	.292	.224	.157	.158	.128
	Std. Dev.	.099	.050	.046	.040	.020
3<V<4 m/sec	Mean	.396	.244	.157	.166	.107
	Std. Dev.	.128	.056	.038	.032	.017
4<V<5 m/sec	Mean	.408	.256	.142	.155	.100
	Std. Dev.	.081	.021	.049	.023	.025
V>5 m/sec	Mean	.447	.267	.137	.153	.093
	Std. Dev.	.010	.012	.028	.009	.012

Table 9. Mean canopy flow coupling indices as computed from
measured wind profiles and their standard
deviations. Two week averages of half hourly data for
seven different months were stratified by the wind
speed at the (46 m) measurement level along the tower.

c.2 Using model wind profiles

An analytical expression for the coupling parameter can be

obtained if explicit forms of the wind profiles above and below

the canopy are assumed. To facilitate comparison of the coupling

efficiency of this tropical forest with other environments, the

formulation suggested by Cionco (1979) was followed. Cionco

assumed a logarithmic wind profile above the canopy and an

exponential profile within the canopy, yielding the following

coupling index:

Figure 15. a) An exponential least-square fit ($R_c = ae^{h/H+b}$) to the mean coupling rations (R_c) as a function of the normalized canopy depth (h/H) for h/H<1. Curve A: Using two-week averaged half-hourly data from all seasons stratified by wind speed at the 46 m level. Curve B: Using two-week averaged half-hourly data, stratified by month. Lower abscissa scale should be used with Curve B.

b) Same as (a), with additional stratification by day (8 a.m. - 6 p.m.) and night.

$$R_C = \frac{u_H \exp\{\alpha(z/H-1)\}}{u_* \, k^{-1} \, \ln(\frac{z-d}{z_O})}$$

where:

u_H - wind speed at canopy top H

u_* - friction velocity $(u_* = \sqrt{\tau/\rho})$

k - von Karman constant

α - canopy flow index or extinction coefficient

d - displacement height

z_O - roughness parameter

The reference levels above and below the canopy were chosen by Cionco as 1.4H and 0.25H. In Cionco's formulation, d was estimated as 0.7H and z_O as 0.14H. For our site z_O, d and u_* were determined previously from observed wind profiles above the canopy (Thompson and Pinker, 1975). The extinction coefficients were computed by Pinker and Moses (1982). Since the 0.25H level used Cionco would be located at the lower canopy, we have chosen as our reference level 0.78H (the lowest measurement level for the upper canopy).

The results presented in Figure 15(A) indicate that in the upper layer of the canopy (0.9H level), the coupling does increase with the ambient wind speed; at the lower levels (0.78H and 0.50H), no systematic dependence on the magnitude of the ambient wind speed is evident; and, at the lowest measurement level (0.133H) a complete reversal occurs, the coupling is highest when the ambient wind is lowest. For additional details see Pinker (1982).

8.   THE TURBULENCE STRUCTURE OF THE FOREST ENVIRONMENT

   a.   Summary

A detailed analysis of the wind structure and its variability in the tropical forest environment was conducted. Special consideration was given to the extraction of information relevant for dispersion modeling. Variability parameters within and above the forest canopy which characterize the dispersion process under different stability conditions were derived. A similar analysis was performed for the nearby clearing (to facilitate comparison between smooth and rough terrain under identical ambient conditions). Detailed results based on a limited sample of data (7 days) were presented in Pinker and Holland (1985). In this report the previous results will be supplemented with information which was derived from a comprehensive data base. Detailed discussion of these results will follow in papers which are being prepared for publication.

   b.   Background

Atmospheric turbulence has been recognized as responsible for the dispersion of suspensoids in the atmosphere. The meteorological conditions that have been related to dispersion are the thermal stability (Slade, 1968) and wind direction fluctuations (Pasquill, 1974).

The most widely used model for estimating the concentration of pollutants from point or area sources is the Gaussian solution of the diffusion equation. The required input parameters are the horizontal σ_y and vertical σ_z distribution of concentration.

Generally, the σ_y and σ_z are not measured but prescribed, after the atmospheric turbulence is characterized in terms of the Pasquill A-F stability classes (Pasquill, 1961; Gifford, 1961), based on measured values of σ_y and σ_z from experiments on dispersion for ground level releases. EPA, however, uses the STAR program (Turner, 1964) to classify turbulence and the U.S. Nuclear Regulatory Commission (NRC, 1974) uses ΔT and σ_v (as detailed in the NRC Safety Guide 1.23). In this scheme a set of ranges of $\Delta T(°C/100\ m)$ and σ_v are related to the A - F classes.

Turbulence over flat terrain has been extensively studied (Lumley and Panofsky, 1964; Panofsky and Dutton, 1984). The data analysis generally consists of ordering the dispersion data by Pasquill stability classes. However, the Pasquill stability classification method does not provide compensation to account for the differences in roughness. For both σ_y and σ_z there is evidence that there is an enhanced initial dispersion near the source due to local roughness elements over what would be predicted from the Pasquill curves. Also, there is evidence that the turbulence structure in a forest canopy has its own characteristics. For modeling purposes, a climatology of turbulence is needed. The data collected during the TREND experiment span almost a whole year. As such, they are most suited to provide information on such aspects of turbulence as height dependence of the horizontal wind fluctuations over and inside a tropical forest canopy and facilitate comparison between rough and smooth terrain under identical ambient conditions. A data sample was selected and an analysis methodology was

developed. It has provided a self-consistent and physically
plausible description of the vertical distribution, in and above
the forest and over the clearing, of the mean wind and
temperature and their turbulent fluctuations. This enabled us to
define limits for the distinguishable regimes in terms of
stability and height and to design with confidence a statistical
analysis program for the larger data set.

c. Procedures and results

In order to characterize the stability conditions over the
forest and the clearing in a coherent manner, several com-
putational experiments were conducted. It seemed that the
32-46 m layer above the forest and the 1-16 m layer above the
clearing exhibit similar response to the external heating, and
develop consistent stability characteristics (Figs. 16a-f). The
diurnal variation of the temperature at the 1 m level in the
clearing, 30 m level at the forest and the wind speed at the 46 m
level in the clearing are also illustrated.

The close parallelism of the 1 m CT and 30 m FT temperature
curves confirm that the air responds in a qualitatively similar
manner to the diurnal radiative cycle and to most of the
superimposed perturbations presumably associated with clouds and
convective disturbances. The lapse rates show a general pattern
as follows. Absolute values are very small in all four layers
during the night hours. During midday the lapse rate becomes
very unstable (negative) in the layer 1-16 m over the clearing,
less so in the layer 32-46 m over the forest, still less so in
the layer 32-46 m over the clearing, and markedly stable

Figure 16. The diurnal variation of the lapse rate (γ) in the 32-46 m layer above the forest and the 1-16 m layer above the clearing; the diurnal variation of the temperature (T) at the 1 m level in the clearing, 30 m level in the forest and the wind speed (W.S.) at the 46 m level in the clearing:

a) for June 20, 1970; b) for June 25, 1985; d) for June 26, 1970; e) for June 27, 1970; f) for June 28.

51

(positive) in the layer 1-16 m in the forest. Disturbances indicated by sharp increases in wind speed with sharp decreases in temperature occurred at about 1200 on day 177 (Fig. 16d) and 1430 on day 179 (Fig. 16f). On both occasions the lapse rates at 1-16 m at CT and FT converged and, in the first case, crossed, the layer within the forest becoming unstable (negative "lapse rate") while at the same heights over the clearing the air became stable as did that above the forest canopy on both occasions.

c.1 Stability classification

The gradient Richardson Number (Ri) defined as:

$$Ri = \frac{g}{\bar{T}} \frac{\partial \bar{\theta}/\partial z}{(\partial u/\partial z)^2}$$

where:

g - acceleration of gravity ($9.8 m/sec^2$)

$\bar{T}$ - average layer temperature in °K

$\bar{\theta}$ - potential temperature

u - mean wind speed at height z

was used for stability classification.

Half hourly averaged data were used. The following 3 stability categories were identified:

	Ri<	-0.03	unstable
-0.03 <	Ri<	0.03	neutral
	Ri>	0.03	stable

To select appropriate height intervals for the evaluation of Ri, we examined time series of Ri in various layers at the FT and CT such as those for which the temperature lapse rates were shown in Fig. 16. It was found that the layers 1-16 m at CT and 32-46 m at FT had nearly parallel and equal Ri time series.

According to the Monin-Obukhov (M-O) similarity theory, assuming horizontal homogeneity and steady state, the standard deviation of vertical and horizontal wind direction fluctuations are functions of z/z_o and z/L, where:

$$L = \frac{-u_* \; c_p \; \rho \bar{T}}{k \; g \; H}$$

L   - the (M-O) length scale

c_p - specific heat at constant pressure

H   - surface heat flux

Since u_* and H are assumed independent of height in the surface boundary layer, L can be also assumed constant with height in this layer. Similarity theory also states that z/L is a function of Ri number only. Several relationships between L and Ri number have been suggested.

According to the Businger-Dyer-Pandolfo empirical results (Businger, 1966; Pandolfo, 1966)

* z/L measures the relative importance of heat convection and mechanical turbulence. If $z/L = 0$, this would indicate that the turbulence is only mechanical.

for neutral cases: $z/L = Ri$

for stable cases: $z/L = \dfrac{Ri}{(1.0-5\ Ri)}$

for unstable cases: $z/L = -\dfrac{Ri}{(Ri\cdot 0.6-1.0)}$

These equations give an estimate of L from measurements of Ri number.

According to Panofsky and Prasad (1965)

$$\sigma_\phi = \frac{\sigma_w}{\bar{u}} = \frac{k\ \phi_3\ (z/L)}{[\ln\ z/z_o - \psi(z/L)]}$$

$$\sigma_\theta = \frac{\sigma_v}{\bar{u}} = \frac{k\ \phi_2(z/L)}{[\ln\ z/z_o - \psi(z/L)]}$$

$\phi 2$, $\phi 3$, ψ – universal functions of stability

c.2 Site parameters

For near-neutral conditions it is assumed that the wind speed variation with height obove the forest canopy is represented by the logarithmic relation:

$$u(z) = u_*/k)\ \ln[(z-d)/z_o]$$

The z_o is estimated graphically as the intercept of the straight line where the mean horizontal wind speed u(z) is

plotted against log (z-d) on a semi-log paper (after establishing d) and u_* is estimated from the slope.

There are several methods to estimate d. In the present study. For each neutral profile we started with a first guess d value of 27 m, performed a least square fit and derived all the micrometeorological parameters. Then, d was incremented by 1 m and the procedure was repeated (Table 10). The d value which yielded the best least square fit was selected along with the corresponding site parameters.

FOREST

Richardson No.: .010   (Neutral)   Z/L: .010   Avg. U: 4.396

d	u_*	z_0	C_d	Error (Y)	Correlation
27.0	.9251	1.9623	.0443	1.0470	.9956
29.0	.7065	.9075	.0258	1.0257	.9992
29.5	.6482	.6864	.0217	1.0162	.9997
30.0	.5866	.4869	.0178	1.0153	.9998
31.0	.4473	.1663	.0103	1.0896	.9964

Table 10. Example of the least square sitting statistics for different values of d and the corresponding site parameters, for a case that was classified as neutral. For this case, the best fit was obtained for d = 30 m.

The resulting statistics for z_0, d and the remaining parameters are presented in Table 11a. In a previous study (Thompson and Pinker, 1975) the approach of Stearns (1970) was adopted for

computing z_O and d. Surface roughness and displacement height were determined so that the error squares on wind speed were a minimum, namely:

$$\varepsilon_i = u_i - u_* k^{-1} [\ln(\frac{z_i + d + z_O}{z_O}) + \phi_i]$$

where ε_i is the error between the measured wind speed at the different z_i levels and the theoretical wind speed at the same height. This least square method (Lettau, 1957; Robinson, 1962) requires that $\sum_{i=1}^{n} \varepsilon_i^2$ is a minimum for n measurement levels. For June, this approach yielded a value of d = 27 m. Had we adopted this latter value of d, the micrometeorological parameters would assume values as presented in Table 11(b).

c.3 Turbulence statistics

c.3.1 Data Processing

The high frequency temperature and wind velocity data were processed to derive mean hourly values of temperature ($\bar{T}$) horizontal wind speed ($\bar{V}$) and direction ($\bar{\theta}$) and horizontal wind speed components ($\bar{u}$; $\bar{v}$). The standard derivations (σ_T; σ_V; σ_θ; σ_u; σ_v) were computed from each hourly mean, using the 360 data points in each sample. The covariance terms $\overline{u'T'}$, $\overline{v'T'}$, $\overline{u'v'}$, $\overline{V'T'}$ and $\overline{\theta'T'}$ were also computed (Table 12). After deriving the average wind speed and direction for each hourly sample, the wind vector for each 10 second was decomposed into along and cross wind components and the σ statistics for these components were also derived. All the turbulence statistics products were

FOREST TOWER		MEAN	ST. DEV.	#CASES
A	displacement height d	30.04	0.79	133
	friction velocity u_*	0.51	0.13	133
	roughness parameter z_o	0.42	0.30	133
	drag coefficient c_D	0.017	0.007	133
	STABILITY PARAMETERS			
	unstable $(z-d)/L$	-0.057	0.023	53
	stable $(z-d)/L$	0.048	0.008	4
	unstable L	-246.7		
	stable L	280.0		
B	displacement height d	27.00		
	friction velocity u_*	0.83	0.196	133
	roughness parameter z_o	1.78	0.340	133
	drag coefficient c_D	0.041	0.009	133
	CLEARING TOWER			
	friction velocity u_*	0.322	0.062	81
	roughness parameter z_o	0.055	0.052	81
	drag coefficient c_D	0.010	0.00156	81
	STABILITY PARAMETERS			
	unstable z/L	-0.1812	0.239	74
	stable z/L	0.0916	0.0775	28
	unstable L	-47.2		
	stable L	92.7		

Table 11. Summary of the micrometeorological parameters for the forest (FT) and clearing (CT) sites obtained from seven days of half hourly averaged observations in June, 1970. a) results obtained when d was selected as yielding the best least square fit to the wind profiles. b) d was selected as the value which minimizes the errors between the model predicted and measured wind speeds at all levels of observation.

HOURLY AVERAGES - DAY: 175   HOUR: 21   MINUTE: 0

Table 12. An example of the turbulence statistics output for each hourly data set. For each measurement level the following is given: the number of observations in each hourly sample; average values of $\bar{T}$, $\bar{V}$, $\bar{u}$, $\bar{\theta}$ and their standard deviations (σ_T, σ_V, σ_u, σ_v, σ_θ) from the hourly mean; the covariances

stored on tapes for possible additional analyses. Only several of these products were analyzed.

Data quality checks were conducted on all the data used. Table 13 illustrates the histograms of the frequency distributions of temperature, wind direction and the u and v components. It seems plausible that the wind direction data for the 32 m level at the forest canopy top and at the 24 m level in the clearing might be in error. This was the case for all seven days investigated. Therefore, these two levels were eliminated from further analyses involving wind direction.

c.3.2 Diurnal variation of σ_V and σ_θ

For each day, the diurnal variation of σ_V and σ_θ was plotted at all eight levels along the forest and clearing towers (Figs. 17-18). There appear to be 3 distinct regimes along the forest tower: 1) levels 46, 40, 36, 32 m 2) level 30 m 3) levels 25, 16, 4 m. The largest standard deviations are found above the canopy, the lowest in the canopy and there is a transition zone along the 30 m level. Therefore, for some of the analyses of variance, only one level from each category will be selected (46, 30, 4 m). In the clearing, the scatter is smaller and so are the σ's. However, within the narrow range of values there is a consistent ordering by level, the smallest values obtained near the ground. For both sites it is evident that the stability and the magnitude of the wind speed affect the variance. The relative maxima are attained during noon-time (unstable conditions) and at night (highest wind speeds).

Table 13. Histograms of the frequency distributions of temperature, wind direction and the u and v components for June 24, 1970, 21:30 p.m. (Such histograms were computed for each hourly sample).

Figure 17a. a)   The diurnal variation of the wind speed standard derivation
                 (σ_V) for all eight (FT) levels, for June 23, 1970.

Figure 17b. Same as Fig. 17a for (CT).

64

Figure 18a. The diurnal variation of the wind direction standard deviation (σ_θ) for all eight (FT) levels for June 23, 1970.

Figure 18b. Same as Fig. 18a for (CT).

Figure 18 presents the standard deviations of the wind direction, σ_θ, along the forest and clearing towers. The values at the 32 m (FT) level seem high and are possibly due to faulty measurements. At the other levels, the σ_θ's seem to fall within a narrow range in which the ordering is reverse than for the wind speed. The smallest values in the wind direction fluctuations are found above the forest while the largest are inside the forest. Some values (e.g., 4 m and 30 m level at night) are exceptionally high and possibly due to the stalling of the instruments at very low wind speeds. On the basis of these plots, it was found appropriate to edit first all the data files of the standard deviations; values that seemed erronous were eliminated (approximately 3%) from subsequent analyses.

c.3.3 Stability effects on turbulence

The effects of the forest on the turbulent kinetic energy can be seen when the vertical profiles of average values of the hourly standard deviation of wind speed, σ_v, for the CT and FT are compared (Fig. 19). The observations have been grouped into stable, unstable and neutral categories as defined in Section 8(c.1). It is seen that in these samples the largest values of σ_v at both sites and at nearly all levels occurred under neutral stability conditions and the smallest under stable conditions.

The pattern over the clearing is that of a smooth increase of σ_v with height above the surface up to a maximum at 24-32 m, then a gradual decrease. In the forest, on the other hand, much

Figure 19. Mean hourly standard deviation of 10-sec wind speed (abscissa) vs. height. a) clearing tower; b) forest tower.

68

smaller values are found up to the top of the canopy, with
profiles from 32 to 46 m above the treetops resembling vertically
compressed versions of the entire CT profiles from 1 to 46 m. At
24 m, where the neutral CT profile has its maximum, the neutral
FT profile has a sharp minimum about 1/7 the CT values,
suggesting a 50-fold reduction of turbulent kinetic energy by the
crown zone relative to the clearing at the same height. Above
the forest canopy the average σ_v values are comparable to those
at the same height above ground at the clearing site although the
mean wind speeds are less over the canopy (Pinker, 1980). Thus
the enhanced roughness of the forest results in greater turbulent
kinetic energy at a given wind speed.

In each stability class, the σ's were plotted as a function
of wind speed at all eight levels along the forest and clearing
towers. The BMDP statistical software as converted for use on
SPERRY 1100 series computers by the University of Utah Computer
Center, was used. Results are illustrated in Fig. 20. As
evident from this figure, the standard deviations increase
linearly with wind speed but the slopes and intercepts vary
according to the measurement level and stability class.

The first-order effects of the forest on the turbulence in
the overlying atmospheric layer, as modulated by stability, are
illustrated in Fig. 21. Here we have selected a level (36 m) at
the forest tower well above the tree tops and a level (16 m)
above the clearing at which the mean wind speed and its diurnal
variation are about the same. The "unstable" stability
classification is subdivided to include a "very unstable"

Figure 20. Scattergrams of hourly standard deviations of 10-sec wind speed vs hourly mean wind speed for different stability classes and at different levels along the forest (FT) and clearing (CT) towers. Results are illustrated for the following cases: a) FT, 36 m, neutral; b) FT, 32 m, neutral; c) FT, 30 m, neutral; d) CT, 8 m, neutral.

PAGE 31 BRDP60 WIND SPEED AND STANDARD DEVIATION DAYS 171, 174-179

```
       .............................................................
 2.0  :                                                            :
      :                                                            :
 1.6  :                              c                             :
      :                                                            :
S     :                                                            :
I 1.2 :                         c    c  c                          :
G     :                       c c  c c                             :
M     :                      cccc                                  :
A     :             c  c    cccc                                   :
S     :            cc   cccc                                       :
 .80  :          cc  cccc                                          :
      :              cccc                                          :
      :            cc                                              :
      :           cccc                                             :
      :          cccc                                              :
 .40  :      c   cc                                                :
      :                                                            :
      :  c                                                         :
 0.0  :                                                            :
       .............................................................
      0.0      .70      1.4      2.1      2.8      3.5      4.2      4.9      5.6
                                                    WINDS
```

N = 176
R = .9405
P(R) 0.000

	MEAN	ST.DEV.	REGRESSION LINE	RES.MS.
X	1.32698	.60840	X= 1.90094*Y-.22814	.01945
Y	.774413	.20116	Y= .463234*X+.19408	.00472

IVAR = 6 WINDS   VS. IVAR = 14 SIGMAS   GROUP=NEUTRALF, SYMBOL=C

PAGE 34 BRDP60 WIND SPEED AND STANDARD DEVIATION DAYS 171, 174-179

```
       .............................................................
 2.0  :                                                            :
      :                                                            :
 1.6  :                                              f   f    f     :
      :                                                 f           :
S     :                                        f    ff   ff         :
I 1.2 :                                 f   f  fff f  f             :
G     :                              ffff                          :
M     :                       f  f  ffff                           :
A     :               f  f  f  ff    fff                           :
S     :            f       f  f                                    :
 .80  :          f       f                                         :
      :          f                                                 :
      :                                                            :
 .40  :                                                            :
      :       .                                                    :
      :                                                            :
      :                                                            :
 0.0  :                                                            :
       .............................................................
      0.0      .70      1.4      2.1      2.8      3.5      4.2      4.9      5.6
                                                    WINDS
```

N = 59
R = .9136
P(R) 0.000

	MEAN	ST.DEV.	REGRESSION LINE	RES.MS.
X	3.1018	.70652	X= .33551*Y-1.1504	.0372
Y	1.1082	.19993	Y= .33551*X+.72266	.0368

IVAR = 6 WINDS   VS. IVAR = 14 SIGMAS   GROUP=NEUTRALC, SYMBOL=F

category.

Figure 21 shows the linear regressions of σ_v on $\bar{V}$ for each stability category at FT (Fig. 21a) and CT (Fig. 21b). It is seen that the linear regressions at these levels all have pronounced and similar slopes and relatively small intercepts, indicating a primary mechanical component of the turbulence as represented by σ_v, dependent on the mean speed. Further, both over the clearing and over the forest, the unstable and very unstable categories produce increasing slopes compared to the neutral and stable categories, suggesting an additive component of turbulence due to buoyancy. Finally, the slopes are consistently greater for all stability categories over the forest than over the clearing, confirming the contribution of the greater surface roughness to the level of turbulent kinetic energy at a given wind speed. These physically plausible relationships are heartening in view of the relatively small samples of data falling into some of the categories.

The positive intercepts show that the relationships are not truly linear, since σ_v must go to zero when $\bar{V}$ goes to zero. If these values are hypothesized to reflect an additive buoyant turbulence component independent of mean speed (or negatively correlated with it), the ordering of the intercepts by stability category does not confirm this.

To obtain a more complete picture of the mechanical turbulence-producing effect of the forest, vertical profiles of the slopes of the linear regressions of σ_v vs $\bar{V}$ for three stability categories are shown in Figure 22. As with σ_v itself,

FOREST TOWER 36m

CLEARING TOWER 16m (JUNE)

Figure 21. Hourly standard deviation of 10-sec wind speed vs hourly mean wind speed. Linear regression curves for four* stability categories. a) clearing tower, 16 m; b) forest tower, 36 m.

the profiles for the clearing site show a smooth vertical variation, in fact an essentially monotonic decrease. Thus the effect of increasing mean wind speed with height must overcome this decreasing coefficient for the observed increase of mean σ_V with height in the lower layers to occur.

Above the canopy top from 30 m to 46 m at the forest site we again see a compressed version of the entire profiles from 1 to 46 m at the clearing but with somewhat larger values of the coefficient consistent with the greater roughness of the forest. Within the forest canopy, however, we see the effect of the trees on turbulence production, the values of the coefficient being some 2 to 5 times larger than those at the same levels over the clearing. There is also the suggestion of an effect of the reversal of stability within the forest relative to that above the forest and over the clearing. Of the three categories the "stable" category, defined by Ri in the layer 32 to 46 m, and essentially a night-time condition, produces the smallest slope of σ_V vs $\overline{V}$ in that layer, but has the largest slope at 3 of the 4 levels below the canopy top. This could be interpreted to mean that more turbulent kinetic energy is generated by the very light winds within the forest canopy when the vertical temperature gradient is destabilized by radiative cooling of the canopy top. Coefficients near unity mean that the turbulent kinetic energy tends to be of the same magnitude as the kinetic energy of the mean flow.

The hypothesis that the quasi-linear curve of σ_V vs $\overline{V}$ will be raised by increasing instability, requiring an increasing

74

Figure 22.   Same as Fig. 19 with slope of linear regression of σ_v vs $\overline{u}$ as abscissa.

75

Figure 22b.

Figure 22c.

additive constant, represented by the intercept of the linear regression (Holland and Myers, 1953), can be re-examined with the vertical profiles of the intercept, shown in Fig. 23. Thus if some part of the increase in turbulent kinetic energy caused by buoyancy were independent of mean wind speed and relatively insensitive to roughness or height above the frictional surface, we should see larger intercepts in the unstable than in the neutral and stable cases, constant or increasing with height. Except in the lowest 24 m over the clearing, no such consistent pattern is found. The intercept does increase with height in each stability category except inside the forest canopy, but the flattening of the regressions with height due to decoupling of the local wind speed and turbulence from the shear and surface stress, especially in the neutral and stable cases must be considered an equally likely explanation.

When the standard deviations are normalized by mean speed, the "intensity of turbulence" $\sigma_v/\bar{V}$ is obtained. Vertical profiles of this quantity are shown in Fig. 24. For the CT, the values decrease smoothly and at similar rates with height for all stabilities, those for the unstable case being consistently the greatest. At the FT, the profiles for the atmospheric layer above the canopy top behaves in a qualitatively similar manner but with larger values, and a more rapid decrease with height similar to those of the linear slope coefficient seen in

Figure 23. Same as Fig. 19 with intercept of linear regression of σ_v vs $\bar{v}$ as abscissa.

Figure 23b.

Figure 23c.

Figure 24. Same as Fig. 19 with average intensity of turbulence $\sigma_v/\bar{v}$.

Figure 2. Below the canopy top, however, turbulence intensities vary in a more irregular manner, generally increasing upward but apparently also reflecting varying canopy density at different levels (Pinker and Moses, 1982). The vertical profiles of σ_u, σ_v and σ_V, normalized by the friction velocity, u_*, are shown in Figure 25 (Values at levels where instruments were suspected to be malfunctioning, were excluded from presentation). Similar profiles for σ_{aw}/u_* and σ_{cw}/u_* are presented in Figure 26. Maitani (1979) presented the nondimentional statistics of turbulence intensities $\sigma_u/\bar{v}$, $\sigma_v/\bar{v}$, $\sigma_w/\bar{v}$ against $(z-d)/z_0$ for different surface types. The reproduced figures (permission of author and publisher were granted) were augmented with our findings, as presented in Figure 27. Our values were derived from data covering February, June and August, 1970. Over the forest, the symbol (f) was used when $z_0 = 170$ cm was assumed and (f') for $z_0 = 45$ cm. Over the clearing, the symbol (c) was used.

c.3.4 Comparison of stability classifications

For the preliminary study, data sets were selected for which, in addition to wind and temperature profiles, information on insolation was also available. This enabled us to establish a correlation between the Pasquill stability classes and the gradient Richardson number, over the forest and the clearing as follows.

Initially, Pasquill stabilities were determined as given by Turner (1959) who related wind speed and the incoming solar radiation during the day and cloudiness at night to the various

83

Figure 25. Same as Fig. 24, normalized by u_*.

Figure 25 cont.

84

Figure 26. Same as Fig. 25 for σ_{AW} and σ_{CW}.

MICROCOPY RESOLUTION TEST CHART
NATIONAL BUREAU OF STANDARDS-1963-A

Figure 26b.

Figure 26c.

Figure 27. Intensities of turbulence versus $(z-d)/z_o$. Symbols:

Δ – Kansas (18 cm wheat stubble);
○ – Hiratsuka (open ocean);
▲ – Tamano (20 cm rice stubble);
× – Hamamatsu (flat soil surface);
○ – Kurashiki -1 (60 cm paddy field);
○ – Kurashiki -2 (90 cm paddy field);
C – Forest clearing in Thailand;
f – Tropical forest Thailand (32 m; z_o = 170 cm);
f' – Tropical forest Thailand (32 m; z_o = 45 cm);
a) $\sigma_u/\overline{V}$; b) $\sigma_v/\overline{V}$; c) $\sigma_w/\overline{V}$

$$\frac{\sigma_v}{U} = 125 \frac{k}{\log(\frac{z-d}{z_o})}$$

Figure 27b.

89

$$\frac{\sigma_w}{U} = 125 \frac{k}{\log(\frac{z-d}{z_0})}$$

c

Figure 27c.

90

strong values - above 1000 mly/min. The wind speeds at 46 meters

for the forest and 24 m for the clearing towers were used. The

justification for this particular selection of levels is

illustrated in Figure 28 which represents the average wind

profiles for the period of study.

Surface Wind Speed (at 10m), m sec^{-1}	Day			Night		
	Incoming Solar Radiation			Thinly Overcast or >4/8 Low Cloud		<3/8 Cloud
	Strong	Moderate	Slight			
< 2	A	A-B	B			
2-3-	A-B	B C	E	F		
3-5	B	B-C	C	D	E	
5-6	C	C-D	D	D	D	
> 6	C	D D	D	D		

Table 14. Key to Stability Categories

The neutral class, D, should be assumed for overcast conditions during

day or night. Subsequently, for each hourly averaged condition the

Richardson numbers were averaged and predicted limits on their range

established by using the formulas given by Sedefian and Bennett (1980)

with values of 1/L from the nomogram of Golder (1972) with the values

of z_o and D from our Table 11. The results are presented in

Table 15. The formulas based on Businger (1973) were used, given as:

Figure 28.   The June seven day average wind profiles along the forest
and clearing towers. The average wind speed at the 46 m
level of the FT approximates the wind speed at the 24 m
level of the CT.

$$Ri = \frac{(z/L)\,\phi_h}{\phi_m^{\,2}}$$

where ϕ_n and ϕ_m are nondimensional temperature and wind profiles, given as:

$$\phi_h = 0.74(1-9\ z/L)^{-1/2}$$

$$\phi_m = (1-15\ z/L)^{-1/4} \qquad z/L<0$$

$$\phi_h = 0.74+4.7\ z/L$$

$$\phi_m = 1+4.7\ z/L \qquad z/L>0$$

Pasquill Class	FT observed	FT from model $z_0 = 42$ cm $D = 30$ m	$z_0 = 178$ cm $D = 27$ m	CT observed	model $z_0 = 5.5$ cm
A					
	-.08	-.38	-.44	-.66	-.52
B					
	-.06	-.09	-.09	-.23	-.14
C					
	-.02	-.009	-.01	-.14	-.03
D					
	+.007	+.02	+.01	+.008	+.02
E					
	+.02	+.05	+.06	+.08	+.08
F					

Table 15. Average observed Ri number (June data only) at each Pasquill class and model derived Ri numbers, using the formulation of Businger (1973) for the nondimensional temperature and wind profiles. Two values for the roughness parameter z_0, over the forest were assumed.

The height was taken as the geometric mean of the lower and upper levels used in the computation of the oberved Ri, i.e. for CT $(1 \text{ m} \quad 16 \text{ m})^{1/2} = 4 \text{ m}$; for FT with D = 30 m, $[(32-30) \text{ m} \quad (46-30) \text{ m}]^{1/2} = 5.6 \text{ m}$ and with D = 27 m, $[(32-27) \text{ m} \quad (46-27) \text{ m}]^{1/2} = 8.9 \text{ m}$.

In order to extrapolate Golder's nomogram from the upper limit of 50 cm for z_O to our value of 178 cm found when D is taken to be 27 m, the 50 cm values of 1/L from the nomogram were multiplied by ln 50/ln 178. It turns out that the increase in z roughly compensates the decrease in 1/L when D = 27 m and z_O = 178 cm are used for the FT in place of D = 30 m and z_O = 42 cm, so that the Ri limits change only slightly. The model values agree with the observed within a factor of five in all cases and within a factor of three in most. This is gratifying in view of the great difference between these limits and those cited in the review of several studies by Sedefian and Bennett (1980). Using a value of z_O = 3 cm with formulas of Businger (1966), Pandolfo (1966), McVehil (1964), Hicks (1975), they gave values ranging as follows:

Stability Class	Range of values of Ri at upper limit
A	-5.6 to -2.5
B	-2.39 to -1.07
C	-.615 to -.275
D	+.089 to +.174
E	+.128 to +.416

Table 16. Range of values for the Ri number upper limit for the Pasquill classes as derived by Sedefian and Bennet (1980), using several formulations of the nondimensional temperature and wind profiles. A roughness parameter z_O = 3 cm was assumed.

Clearly the increased roughness results in a much narrower range of Richardson numbers (or of values of 1/L) than is found over grassland. Although based on a small sample our results suggest that Golder's nomogram can be extended to larger z_O values and lend support to the use of 1/L or Ri to classify observations by Pasquill stability categories.

In order to establish limits on the Ri number for each Pasquill stability class as observed over this tropical forest, we selected cases for which all the necessary information was available to determine independently the Ri number and the Pasquill stability class. In Figure 29, each case is displayed indicating the corresponding Pasquill stability class. As evident, there is some overlap between the different classes. In order to establish statistically sound limits on the Ri number appropriate for each stability class, we compiled a frequency distribution of the number of cases in each category (Table 17a). The values on the left represent the upper limit on the Ri number. The upper and lower limits for each class are given in Table 17b and were subsequently inserted into Fig. 28.

c.3.5 Comparison of   's over different terrain

Over plant canopies, the fluctuations of vertical and horizontal wind directions play an important role in the turbulent diffusion of particulates. While fluctuations of wind speeds have been more frequently studied (Inoue et al., 1975; Maitani, 1977), fewer studies have been conducted on wind direction fluctuations. It is the horizontal wind direction fluctuation which is required as input for models on lateral

Figure 29. The distribution of the stability according to independently derived Ri numbers and Pasquill classes for a sample covering February June and August, 1970.

96

Figure 29. Continued.

FOREST

Pasquill Class	A	B	C	D	E	F
Ri up.lim. <						
-.15	9	7				
-.04	9	61	25	1		
-.01		10	65	3		
+.01			29	305	6	
+.05				19	53	4
>					5	17

CLEARING

Pasquill Class	A	B	C	D	E	F
Ri up. lim. <						
-.50	16	2				
-.16	3	56	23	2		
-.04		14	74	10		
+.04			9	283	15	
+.34				23	89	6
>					3	6

RICHARDSON NUMBER LIMITS

Pasquill Class	FT	CT
A	Ri < -.15	Ri < -.50
B	-.15 < Ri < -.04	-.50 < Ri < -.16
C	-.04 < Ri < -.01	-.16 < Ri < -.04
D	-.01 < Ri < .01	-.04 < Ri < .04
E	.01 < Ri < .05	.04 < Ri < .34
F	Ri > .05	Ri > .34

Table 17. Frequency distributions of the number of cases in each Pasquill class and in a certain interval of Ri numbers (A), serving as a basis for establishing the upper and lower limits on the Ri number for each Pasquill class (B).

dispersion. Selected information on   obtained for the forest

and clearing environments (using June data) was extracted and

compared with results from other studies conducted over different

surface types. In Table 18, the average   's at the top of the

forest and clearing towers are presented for each Pasquill

stability class. For comparison purposes, the values obtained by

Sadhuram and Vittal Murthy (1983) (S-V), Padmanabha Murthy and

Gupta (1979) (P-G) and Shirvaikar (1975) (S) are indicated. (S-

V) studied the seasonal variation of   over the complex terrain

of a coastal city situated on the Bay of Bengal. The wind

direction measurements used in their investigation were taken at

22 m above the ground with a Dines P.T. Anemometer (whose

sensitivity was not specified). The values of   are determined

from the continuous wind direction trace of 10 years of data

(1958-1967), extracted for 4 typical months only, represented

seasonal variability. (P-G) computed   values over flat terrain

and the values of (S) were obtained for a flat coastal site. All

the three studies report values lower than given by Slade (1968)

or obtained in our study over the clearing. It is possible that

this is due to the instrument limitations used in those

studies. The good agreement between our values over the clearing

and those given by Slade would give confidence also in the values

derived over the forest which are about 30-50% higher than over

the clearing. (Information on   's over forest of the type

obtained during the TREND project is not available from other

sites.) Subsequently, these results were supplemented with

computations based on a more comprehensive data base

(Table 19). The computations were extended to include statistics on $\frac{-}{V}$; $\frac{-}{v}$; $\frac{-}{u}$; $_{cw}$ and $_{aw}$, all as a function of Pasquill stability classes. This was done to enable comparisons with other investigators some of whom present results on the u and v components of the horizontal wind velocity while others compute the along and cross wind components.

Values in degrees

Pasquill Stability	CT June	FT June	S-V Jan	S-V Apr	S-V Aug	S-V Oct	P-G 2.5 m	P-G 20 m	Slade	S
A	35.8	50.4	16	17	12	14	14	14	25	10
B	22.7	31.9	12	13	10	10	12	10	20	7
C	16.5	24.1	8	9	7	8	10	8	15	5
D	9.7	23.6	6	8	7	7	8	6	10	4
E	9.5	21.3	6	6	5	6	6	4	5	2
F	-	-	4	6	4	4	4	2	2	2

Table 18. Comparison of σ_θ's over the forest and clearing with those obtained by other investigators for the Pasquill classes (S-V: Sadhuran and Vittal Murthy (1983); P-G: Padmanabha Murthy (1979); Slade (1968); S: Shirvaikar (1975).

c.3.6 Wind direction shear

In Table 20 the average direction shear for 1 m to 46 m at the CT and for 4 to 30 m and 30 to 46 m at the FT, stratified by stability and also by day vs night is presented.

As shown by Smith et al. (1972) the turning of the wind above a forest canopy (z_o 1m) from the geostrophic wind direction is considerably greater than that over a grassy field,

CLEARING TOWER: 46 m level; February, 1970

	σ_θ Mean	σ_θ S.D.	Ri Mean	$\sigma_{\bar{v}}$ Mean	$\sigma_{\bar{v}}$ S.D.	$\sigma_{\bar{u}}$ Mean	$\sigma_{\bar{u}}$ S.D.	$\sigma_{\bar{v}}$ Mean	$\sigma_{\bar{v}}$ S.D.	σ_{cw} Mean	σ_{cw} S.D.	σ_{aw} Mean	σ_{aw} S.D.	Z/L Mean	# Cases
A	43.3	22.9	-1.52	0.9	.27	1.0	.41	1.3	.34	1.2	.46	1.3	.55	-.79	11
B	27.0	14.0	-.42	1.3	.29	1.5	.42	1.5	.40	1.6	.58	1.5	.40	-.32	20
C	15.7	3.7	-.21	1.1	.42	1.2	.44	1.3	.50	1.3	.52	1.2	.43	-.19	22
D	8.3	3.5	.03	1.0	.24	1.0	.25	1.0	.27	1.0	.29	1.0	.24	.04	75
E	7.0	3.0	.22	0.8	.25	0.8	.24	0.7	.20	0.6	.22	0.8	.24	.34	31
F	9.6	3.5	.95	0.3	.07	0.4	.07	0.3	.00	0.4	.14	0.3	.00	1.90	2

FOREST TOWER: 46 m level; February, 1970

	σ_θ Mean	σ_θ S.D.	Ri Mean	$\sigma_{\bar{v}}$ Mean	$\sigma_{\bar{v}}$ S.D.	$\sigma_{\bar{u}}$ Mean	$\sigma_{\bar{u}}$ S.D.	$\sigma_{\bar{v}}$ Mean	$\sigma_{\bar{v}}$ S.D.	σ_{cw} Mean	σ_{cw} S.D.	σ_{aw} Mean	σ_{aw} S.D.	Z/L Mean	# Cases
A	49.9	23.2	-.26	0.9	.44	1.0	.54	1.2	.49	1.3	.59	11	.53	-.19	7
B	30.3	7.3	-.09	1.1	.35	1.2	.39	1.3	.44	1.3	.53	1.3	.36	-.08	23
C	21.2	6.5	-.02	1.3	.45	1.3	.50	1.4	.45	1.4	.49	1.3	.49	-.02	27
D	10.7	3.2	.01	1.2	.27	1.2	.28	1.0	.30	1.0	.28	1.2	.27	.01	86
E	10.5	3.3	.06	0.6	.17	0.6	.19	0.5	.13	0.5	.14	0.6	.18	.07	21
F	8.6	4.4	.09	0.4	.09	0.4	.10	0.1	.40	0.4	.08	0.4	.12	.19	9

Table 19. A summary of turbulence statistics over the clearing and forest, as a function of the Pasquill classes for: a) February; b) April-May; c) June and d) August, 1970.

CLEARING TOWER: 46 m level; April-May, 1970

	σ_θ Mean	σ_θ S.D.	R1 Mean	$\sigma_{\bar{v}}$ Mean	$\sigma_{\bar{v}}$ S.D.	σ_u Mean	σ_u S.D.	σ_v Mean	σ_v S.D.	σ_{cw} Mean	σ_{cw} S.D.	σ_{aw} Mean	σ_{aw} S.D.	Z/L Mean	# Cases
A	20.1	15.7	-1.52	0.7	.5	0.9	.41	0.7	.25	0.7	.46	0.8	.31	-.75	37
B	18.6	12.1	-.25	1.2	.33	1.2	.41	1.2	.43	1.2	.52	1.2	.52	-.22	22
C	12.6	7.8	-.10	1.3	.29	1.3	.31	1.2	.41	1.1	.47	1.3	.30	-.10	21
D	10.8	8.1	.01	1.2	.38	1.2	.41	1.2	.36	1.1	.50	1.2	.38	.02	47
E	9.4	4.4	.14	1.0	.24	1.1	.39	1.0	.34	1.0	.50	1.0	.26	.26	96
F	10.2	5.2	.89	0.9	.51	0.8	.41	0.8	.38	0.7	.44	0.8	.46	1.80	35

FOREST TOWER: 46 m level; April-May, 1970

	σ_θ Mean	σ_θ S.D.	R1 Mean	$\sigma_{\bar{v}}$ Mean	$\sigma_{\bar{v}}$ S.D.	σ_u Mean	σ_u S.D.	σ_v Mean	σ_v S.D.	σ_{cw} Mean	σ_{cw} S.D.	σ_{aw} Mean	σ_{aw} S.D.	Z/L Mean	# Cases
A	33.2	8.3	-.25	0.8	.07	1.0	.07	1.0	.07	1.0	.07	1.0	.07	-.22	2
B	26.7	7.8	-.07	1.3	.39	1.4	.41	1.3	.47	1.4	.39	1.4	.44	-.07	9
C	20.6	9.2	-.02	1.4	.35	1.5	.35	1.2	.41	1.3	.39	1.5	.39	-.02	18
D	18.8	7.3	.01	1.2	.28	1.4	.38	1.5	.62	1.5	.60	1.4	.42	.01	110
E	16.0	6.8	.03	1.0	.33	1.1	.41	1.0	.49	1.0	.52	1.0	.39	.04	79
F	14.0	4.1	.18	0.6	.24	0.7	.28	0.6	.27	0.5	.32	0.7	.27	.23	63

Table 19b.

CLEARING TOWER: 46 m level; June, 1970

	σ_θ Mean	σ_θ S.D.	Ri Mean	$\sigma_{\bar{V}}$ Mean	$\sigma_{\bar{V}}$ S.D.	$\sigma_{\bar{u}}$ Mean	$\sigma_{\bar{u}}$ S.D.	$\sigma_{\bar{v}}$ Mean	$\sigma_{\bar{v}}$ S.D.	σ_{cw} Mean	σ_{cw} S.D.	σ_{aw} Mean	σ_{aw} S.D.	Z/L Mean	# Cases
A	30.0	6.1	-.51	1.1	.23	1.3	.24	1.4	.35	1.4	.34	1.2	.22	-.38	6
B	18.7	3.9	-.19	1.3	.25	1.3	.23	1.4	.26	1.3	.24	1.3	.26	-.17	27
C	16.2	5.8	-.10	1.2	.21	1.2	.25	1.3	.34	1.2	.36	1.2	.23	-.09	29
D	9.3	2.0	.01	1.3	.24	1.2	.21	1.2	.22	1.1	.20	1.3	.25	.02	67
E	9.0	2.3	.05	1.1	.21	1.1	.20	1.0	.15	0.9	.20	1.1	.22	.10	22
F	9.0	-	.13	1.1	-	1.1	-	0.7	-	0.7	-	1.1	-	.34	1

FOREST TOWER: 46 m level; June, 1970

	σ_θ Mean	σ_θ S.D.	Ri Mean	$\sigma_{\bar{V}}$ Mean	$\sigma_{\bar{V}}$ S.D.	$\sigma_{\bar{u}}$ Mean	$\sigma_{\bar{u}}$ S.D.	$\sigma_{\bar{v}}$ Mean	$\sigma_{\bar{v}}$ S.D.	σ_{cw} Mean	σ_{cw} S.D.	σ_{aw} Mean	σ_{aw} S.D.	Z/L Mean	# Cases
A	50.4	5.7	-.08	1.2	.25	0.9	.76	1.5	.40	1.1	1.00	1.5	.06	-.08	3
B	31.9	8.6	-.06	1.2	.21	1.5	.37	1.4	.27	1.3	.28	1.5	.37	-.06	28
C	24.1	7.2	-.02	1.2	.22	1.4	.32	1.3	.34	1.3	.35	1.4	.32	-.02	41
D	23.6	8.0	.01	1.4	.23	1.8	.45	1.6	.45	1.6	.43	1.8	.44	.01	75
E	21.3	8.7	.02	1.0	.17	1.2	.23	1.0	.21	1.0	.21	1.2	.23	.03	5
F	-	-	-	-	-	-	-	-	-	-	-	-	-	-	0

Table 19c.

CLEARING TOWER: 46 m level; August, 1970

	σ_θ Mean	σ_θ S.D.	Rl Mean	$\sigma_{\bar{v}}$ Mean	$\sigma_{\bar{v}}$ S.D.	$\sigma_{\bar{u}}$ Mean	$\sigma_{\bar{u}}$ S.D.	$\sigma_{\bar{v}}$ Mean	$\sigma_{\bar{v}}$ S.D.	σ_{cw} Mean	σ_{cw} S.D.	σ_{aw} Mean	σ_{aw} S.D.	Z/L Mean	# Cases
A	28.2	15.8	-1.12	1.1	.23	1.0	.18	0.9	.16	0.8	.18	1.1	.16	-.64	4
B	22.7	6.9	-.23	1.3	.26	1.3	.30	1.3	.24	1.4	.39	1.4	.28	-.20	32
C	18.8	7.5	-.09	1.3	.30	1.4	.33	1.3	.37	1.3	.39	1.4	.34	-.08	62
D	11.0	4.3	.02	1.3	.19	1.2	.24	1.2	.22	1.2	.24	1.3	.21	.02	164
E	10.0	4.2	.09	1.1	.40	1.0	.37	1.0	.34	0.9	.26	1.1	.42	.21	57
F	11.2	3.6	.36	1.0	.62	0.8	.38	0.9	.45	0.5	.17	1.0	.62	1.10	9

FOREST TOWER: 46 m level; August, 1970

	σ_θ Mean	σ_θ S.D.	Rl Mean	$\sigma_{\bar{v}}$ Mean	$\sigma_{\bar{v}}$ S.D.	$\sigma_{\bar{u}}$ Mean	$\sigma_{\bar{u}}$ S.D.	$\sigma_{\bar{v}}$ Mean	$\sigma_{\bar{v}}$ S.D.	σ_{cw} Mean	σ_{cw} S.D.	σ_{aw} Mean	σ_{aw} S.D.	Z/L Mean	# Cases
A	35.1	9.2	-.15	1.1	.13	1.1	.41	1.0	.39	1.0	.39	1.1	.43	-.14	9
B	31.4	8.6	-.06	1.2	.26	1.3	.30	1.2	.31	1.3	.31	1.3	.31	-.06	35
C	25.4	6.9	-.02	1.4	.26	1.5	.30	1.3	.28	1.3	.29	1.5	.31	-.02	57
D	16.8	6.1	.01	1.4	.25	1.5	.34	1.3	.34	1.3	.31	1.6	.34	.01	171
E	15.5	5.5	.03	1.0	.31	1.1	.35	0.9	.28	0.8	.29	1.1	.34	.04	38
F	14.8	6.2	.09	0.9	.28	0.9	.25	0.6	.16	0.6	.10	0.9	.32	.22	12

Table 19d.

Wind Direction Shear

	# Cases	Mean (Degree)	St. Dev. (Degree)
FT (46-30 m)			
All	140	32.00	9.64
N	93	32.08	6.70
U	44	30.40	10.30
S	2	31.00	
D	74	32.19	9.39
N	63	31.67	9.88
FT (30-4 m)			
All	128	12.80	23.00
N	82	12.94	24.90
U	44	14.10	23.40
S	2	18.50	
D	72	15.03	24.6
N	52	11.73	23.8
CT (46-1 m)			
All	157	7.11	9.84
N	65	5.00	6.38
U	60	5.60	9.61
S	32	14.25	12.70
D	76	5.50	9.68
N	77	7.84	8.54

Table 20. Mean hourly wind direction shear and its standard deviation in the specified layers of the forest and clearing for the seven June days. N - neutral; U - unstable; S - stable; D - day; N - night.

particularly, under stable conditions (35-40°). Within the forest canopy they point out that the turning depends upon the forest parameters as well as upon meteorological conditions, and is subject to great variability. They predicted a direction shear of the order of 30° in a pine forest and found a mean value of 27° in 385 hours of data with a large standard deviation (20°).

Although we have not computed geostrophic winds, we find an average direction shear between the average canopy top (30 m) and the 46 m level over the forest of 32° (140 hours of data) compared with 7° between the surface (1 m) and 46 m over the clearing (157 hours of data), with standard deviation of 10° at both sites. Within the canopy we find an additional turning of 13° (128 hours of data), smaller than that found by Smith et al., but with a comparable standard deviation (23°).

The effect of stability appears to be in the expected sense at the CT. Above and within the forest, however, because of the small samples and large standard deviations this effect can not be established with significance in the present analysis.

9. Summary

Project TREND (Tropical Environmental Data) was sponsored by the Advanced Research Project Agency (ARPA) and was carried out under the management of the Earth Science Laboratory, U. S. Army Natick Laboratories, Natick, Massachusetts, in the late sixties. The wealth of micrometeorological data that resulted from this project constitutes a valuable resource of great importance. Under project TREND, the most complete set of micrometeorological data in humid tropics was collected and it is doubtful whether any comparable program will be conducted for many years.

The analyses conducted with the data have attested to the high quality and reliability of the data, and resulted in a wealth of information which is slowly finding its way into the literature. Though numerous analyses of the data were conducted and published, still a lot remains to be learned from this rich resource.

ACKNOWLEDGEMENTS

REFERENCES

ASRCT, 1967: Semi-Annual Report No. 1, Cooperative Research Programma No. 27, (TREND), ARPA. Applied Scientific Research Corporation of Thailand, Bangkok.

Allen, C. W., 1958: Astrophysical Quantities. University of London Press.

Angstrom, A., 1925: The albedo of various surfaces of ground. Geograf. Ann., 7, 323-342.

Angstrom, A. K., and A. J. Drummond, 1961: Basic concepts concerning cutoff glass filters used in radiation measurements. J. Meteor., 18, 429-431.

Bahm, R. J., and J. C. Nakos, 1979: The calibration of solar radiation measuring instruments. Final report, Bureau of Engineering Research, University of New Mexico. Report No. BER-1(79) DOE-684-1.

Businger, J. A., 1966: Transfer of heat and momentum in the atmospheric layer. Prog. Arct. Heat Budget and Atmospheric Circulation, Santa Monica, CA, Rand Corp., 305-332.

Cionco, R. M.: A summary of an analysis of canopy flow coupling for a variety of canopy types. Fourteenth Conference on Agriculture and Forest Meteorology, Minneapolis, MN, April 2-6, 1979, AMS.

Cionco, R. M., 1965: A mathematical model for air flow in a vegetative canopy. J. Appl. Meteor., 4, 517-522.

Cionco, R. M., 1972: A wind profile index for canopy flow. Boundary Layer Meteorol., 3, 255-263.

Cionco, R. M., 1978: Analysis of canopy index values for various canopy densities. Boundary Layer Meteorol., 15, 8--93.

Coulson, K. L., 1975: Solar and Terrestrial Radiation, Methods and Measurements. Academic Press.

Dalrymple, P. C., 1975: A comprehensive summary of project TREND. U. S. Army Engineer Topographic Laboratories, Fort Belvoir, VA 22060.

Gates, D. M., H. G. Keegan, J. C. Scheleter and V. R. Weidner, 1965: Spectral properties of plants. Appl. Opt., 4, 11-20.

Gifford, F. A., 1976: Turbulent diffusion-typing schemes: A review. Nucl. Saf., 17, 68-86.

Gifford, F. A., 1961: Use of routine meteorological observations for estimating atmospheric dispersion. Nucl. Saf., 2, 47-51.

Golden, D., 1972: Relations among stability parameters in the surface layer. Boundary-layer Meteorology, 3, 47-58.

Hicks, B. B., P. Hyson and C. J. Moore, 1975: A study of eddy fluxes over a forest. J. Appl. Meteorol., 14, 58-66.

Holland, J. Z. and R. F. Myers, 1953: A Meteorological Survey of the Oak Ridge Area, U. S. Atomic Energy Commission document ORO-99, Oak Ridge, TN.

Inoue, E., 1963: On the turbulent structure of airflow within crop canopies. J. Met. Soc. Japan, Ser. 2, 41, 317-326.

Inoue, K., Z. Uchijima, T. Horie, S. Iwakiri, 1975: Studies of energy and gas exchange within crop canopies (10). J. Agric. Meteorol., 31, 71-82.

Johnson, F. S., 1954: The solar constant. J. Meteor., 11, 431-439.

Joseph, J. H., W. J. Wiscombe and J. A. Weinman, 1976: The delta-Eddington approximation for radiative flux transfer. J. Atmos. Sci., 33, 2452-2459.

Lettau, H. H., 1957: Computation of Richardson's Numbers, Classification of Wind Profiles and Determination of Roughness Parameters. Exploring the Atmosphere's First Mile, Vol. I (ed. by Lettau and Davidson), Pergamon Press, Inc., New York and London, pp. 337-372.

Lumley, J. L. and H. A. Panofsky, 1964: Structure of Atmospheric Turbulence, Wiley, New York.

Maitani, T., 1977: On the downward transport of turbulent kinetic energy in the surface layer over plant canopies. Boundary-Layer Meteorol., 14, 571-584.

Manes, A., and J. H. Joseph, 1978: A numerical procedure for determining atmospheric turbidity indices from pyrheliometric data. Arch. Met. Geoph. Biokl., Ser. B, 26, 29-44.

Mani, A., O. Chacko, and G. Hariharan, 1969: A study of Angstrom's turbidity parameters from solar radiation measurements in India. Tellus, 21, 829-843.

McVehil, G. A., 1964: Wind and temperature profiles near the ground in stable stratification. Quart. J. Roy. Meteor. Soc., 90, 136-146.

Nuclear Regulatory Commission (formerly U.S. Atomic Energy Commission) 1972: Safety guides for water cooked nuclear power plants, Safety Guide 23: Onsite Meteorological Programs, pp. 23.1-23.6, USAEC, Division of Reactor Standards, Washington, DC 20545.

Padmanabha, Murthy B. and R. N. Gupta, 1979: Stability classification in Micrometeorology. Maussam, 30, 526-527.

Paltridge, G. W. and C. M. R. Platt, 1976: Radiative processes in meteorology and climatology. Elsevier Sci. Publ. Co., N.

Pandolfo, J. P., 1966: Wind and temperature for constant flux boundary layers in lapse conditions with a variable eddy conductivity to eddy viscosity ration. J. Atmos. Sci., 23, 495-502.

Panofsky, H. A. and B. Prasad, 1965: Similarity Theories and Diffusion. Int. J. Air Water Poll., 9, 419-430.

Panofsky, H. A., 1973: Tower micrometeorology, In Workshop on Micro-meteorology, (Edited by Haugen D. A.), pp. 151-176. American Meteorological Society, Boston, MA.

Panofsky, H. A., and J. A. Dutton, 1984: Atmospheric Turbulence Models and Methods for Engineering Applications. A Wiley-Interscience Publication, pp. 397.

Pasquill, F., 1976: Atmospheric dispersion parameters on Gaussian plume modeling - II. Possible requirements for change in the Turner workbook values. EPA-600(4-76-0306.)

Pasquill, F., 1961: Atmospheric Diffusion, 2nd Edn., Wiley, New York, 429 pp.

Pasquill, F., 1961: The estimation of the dispersion of windborne material. Met. Mag., 90, 33-49.

Pinker, R. T., O. E. Thompson and T. F. Eck, 1980: The energy balance of a tropical evergreen forest. J. Appl. Meteor., 19, No. 12, 1341-1350.

Pinker, R. T. and J. F. Moses, 1982: On the canopy flow index of a tropical forest. Meteorology, 22, 313-324.

Pinker, R. T., 1982: On the canopy coupling index. Boundary Layer Meteorology, 26, 305-311.

Pinker, R. T., 1982: The diurnal asymmetry in the albedo of tropical forest vegetation. Forest Sci., 28, 297-304.

Pinker, R. T. and R. Kaylor, 1982: Data reduction summary for project TREND (User's Manual), Part I:: "D" Tapes. Publication No. 82-157, Department of Meteorology, University of Maryland, College Park, MD 20742.

Pinker, R. T. and T. F. Eck, 1982: Radiometric measurements of atmospheric turbidity in Thailand. Publication No. 82-196, Department of Meteorology, University of Maryland, College Park, MD 20742.

Pinker, R. T., O. E. Thompson and T. F. Eck, 1980: The Albedo of a Tropical Forest. Quart. J. Roy. Meteorol. Soc., 106, 551-558.

Pinker, R. T., 1980: The Microclimate of a Dry Tropical Forest. Agric. Meteorol., 22, 249-265.

Pinker, R. T., and R. Kaylor, 1982: Data Reduction Summary for Project TREND (User's Manual). Part I: "D" Tapes. Publication No. 92-197, Department of Meteorology, College Park, MD 20742, pp. 116.

Robinson, S. M., 1962: Computing wind profile parameters. J. Atm. Sci., 19, 189-190.

Sahhuram, Y. and Vittal Murthy K.P.R., 1983: Seasonal variation of wind direction fluctuation vs Pasquill Stabilities in complex terrain. Boundary-Layer Meteorol., 26, 197-202.

Sedefian, L. and E. Bennett, 1979: A comparison turbulence classification schemes. Atmospheric Environment, 14, 741-750.

Shaw, R., 1977: Secondary wind speed maximum inside plant canopies. J. Appl. Meteorol., 16, 514-521.

Shinn, J. H., 1971: Steady state two dimensional flow in forests and the disturbance of surface layer flow by a forest wall. R & D Technical Report ECOM-5583, Atmospheric Sciences Laboratory, White Sands Missile Range, NM.

Shirvaikar, V. V., 1975: Recommended Code of Practice for Micro Meteorological Techniques in Air Pollution, ISI. DOC. CDC. 53(6358).

Silbert, M. N., 1970: A structured fluids approach to canopy flow. New York University, School of Engineering and Science, Department of Meteorology and Oceanography, Geophysical Sciences Laboratory TR-70-2.

Slade, H. D., 1968: Meteorology and Atomic Energy, U. S. Atomic Energy Commission, USAEC-TID-24190.

Smith, F. B., D. J. Carson and H. R. Oliver, 1972: Mean wind - direction shear through a forest canopy. Boundary-Layer Meteorol., 3, 178-190.

Stearns, C. R., 1970: Determining Surface Roughness and Displacement Height. Boundary-Layer Meteorol., 1, 102-111.

Stewart, J. B., 1971: The albedo of a pine forest. Quart. J. R. Met. Soc., 97, 561-564.

Tan, H. S. and S. C. Ling, 1963: Quasi-steady micro-
meteorological atmosphere boundary layer over a wheat
field. The energy budget at the earth's surface: Part II:
Studies at Ithaca, NY. 1960 Production Research Report NO.
72, Agricultural Research Serville, Ithaca, NY, 7-12.

Thompson, O. E., and H. E. Landsberg, 1975: Climatological
conditions in the Sakaerat Forest, Thailand. Geografiska
Annaler, 3, - 4, Ser. A, 243 - 260.

Thompson, O. E. and R. T. Pinker, 1975: Wind and Temperature
Profile Characteristics in a Tropical Evergreen Forest in
Thailand. Tellus, 27, 562-573.

Thompson, O. E. and R. T. Pinker, 1981: An error analysis of the
Thornthwaite-Holzman Equation. J. Appl. Meteor., 20, No. 3,
250-254.

Turner, D. B., 1964: A diffusion model for an Urban Area. J.
Appl. Met., 3, 83-91.

Turner, B. D., 1959: Workbook of Atmospheric Dispersion
Estimates. U.S. Dept. of Health, Education and Welfare,
5-29.

APPENDIX A

Publications Based on Information from Project TREND

A. Refereed

Thompson, O. E. and H. E. Landsberg (1975): Climatological
    conditions in the Sakaerat Forest, Thailand. Geografiska
    Annaler, Vol. 3-4, Ser. A, 247-260.

Thompson, O. E. and R. T. Pinker (1975): Characteristic
    temperature spectra in a tropical dry evergreen forest in
    Thailand. Tellus 27, No. 6, 562-573.

Pinker, R. and H. E. Landsberg (1976): Characteristic
    temperature spectra in a tropical dry evergreen area.
    Archives for Meteorology, Geophysics, and Bioclimatology,
    Ser. B24, 243-251.

Pinker, R. T. (1980): The microclimate of a dry tropical
    forest. Agricultural Meteorology, 22, 249-265.

Pinker, R. T., O. E. Thompson, and T. F. Eck (1980): The albedo
    of a tropical forest. Quart. J. Roy. Meteor. Soc., 106,
    551-558.

Pinker, R. T. and O. E. Thompson (1981): An error analysis of
    the Thornthwaite-Holzman Equation. Jour. of Applied Meteor.,
    20, No. 3, 250-254.

Pinker, R. T., O. E. Thompson and T. F. Eck (1980): The energy
    balance of a tropical evergreen forest. Jour. of Applied
    Meteor., 19, No. 12, 1341-1350.

Pinker, R. T. and J. F. Moses (1982): On the canopy flow index
    of a tropical forest. Boundary-Layer Meteorology, 22,
    313-324.

Pinker, R. T. (1983): On the canopy coupling index. Boundary-
    Layer Meteorology, 26, 305-311.

Pinker, R. T. (1982): The diurnal asymmetry in the albedo of
    tropical forest vegetation. Forest Sci., 28, 297-304.

Pinker, R. T. (1985): On the kinetic energy spectra above and
    inside a forest environment. In preparation.

Pinker, R. T. and J. Z. Holland (1985): The turbulence structure
    of a tropical forest environment. In preparation.

Pinker, R. T. and J. Z. Holland (1985): A climatology of the
    dispersion parameters over rough terrain. In preparation.

Pinker, R. T. (1985): The radiation climate above and inside a
    tropical forest canopy. In preparation.

116

B. Recent Technical Notes

Pinker, R. T. and R. Kaylor (1982): Data Reduction Summary for
    Project TREND (User's Manual), Part I: "D" Tapes.
    Publication No. 82-157, Department of Meteorology, University
    of Maryland, College Park, MD 20742.

Pinker, R. T. and R. Kaylor (1983): Data Reduction Summary for
    Project TREND (User's Manual). Part II: "A" Tapes.
    Publication No. 83-198, Department of Meteorology, University
    of Maryland, College Park, MD 20742.

Pinker, R. T. and T. F. Eck (1982): Radiometric measurements of
    atmospheric turbidity in Thailand. Publication No. 82-196,
    Department of Meteorology, University of Maryland, College
    Park, MD 20742.

Pinker, R. T. and J. Z. Holland (1985): Turbulence structure of
    a tropical evergreen forest. Preliminary Report, SR-85-14,
    Department of Meteorology, University of Maryland, College
    Park, MD 20742.

Pinker, R. T. (1984): The ultra-violet radiation climate of a
    tropical forest environment. SR-84-3, Department of
    Meteorology, University of Maryland, College Park, MD 20742.

APPENDIX B

DATA REDUCTION AND STATUS SUMMARY

The micrometeorological data collected during project TREND
were logged on a system capable of analogue and digital
recording. Data recorded on the digital system are referred to
as "D" tape data. Those recorded on the analogue system are
referred to as "A" tape data. A brief summary of the data
reduction process and an inventory of the final product, will
follow.

PROCESSING OF THE TREND EXPERIMENT "A" TAPES

The parameters stored originally on the "A" tapes were:
humidity; rainfall; pressure; radiation; and wind direction. Two
data reduction programs were written by the Watervliet A.R.S.
computer science office for the analog "A" data tapes. The first
program ("Ansec"), edited the data, averaged over 30 minute
intervals, and generated a set of new tapes. At the same time,
the wind direction data were stripped from the original tapes and
written directly to a new set of tapes. A second program
("Pranc"), was designed to read the averaged tapes, relating
instruments to channel numbers, and providing calibration factors
for the radiation instruments which were provided separately on
thousands of cards. At the University of Maryland, the "Pranc"
program was extensively rewritten so that the instruments were
separated by type, and the results written onto six new tapes in
a Fortran readable format. One tape contains only dewpoint data;

117

the second tape contains rainfall, pressure, miscellaneous instruments, and voltage calibrations; the third tape contains radiation data in separate files for longwave (with blackbody temperature) and shortwave radiation. Each instrument is written to a specific entry in an ordered list for output. Thus, the new tapes can be read and the desired instruments isolated, without requiring the control data deck necessary with the "Pranc" program. Channel numbers and alpha numeric identities are still retained in the output so that filter changes or other modifications to the instruments may be traced back to the original log books. Each of the new output tapes has a format suited to the data contained on it and, end-of-file marks were inserted after the data corresponding to each original "A" input tape. Calibrations used for the radiation instruments are those that were supplied on the "Pranc" control data cards. Output tapes are written in Univac formatted Fortran output, and as such, readable only on a Univac machine. However, tapes in a card image format could be produced, if necessary.

The newly generated tapes are stored at the Department of Meteorology, University of Maryland, under the internal tape numbers:

> P5995; P5870 (Radiation)
>
> P5994; P5813 (Dewpoint)
>
> P4336; P5814 (Rainfall, Pressure and Voltage).

For more details see Pinker and Kaylor, (1983a).

PROCESSING OF THE "D" TAPES: ('PACK')

Our original repacking program of the raw data produced a packed binary tape, with five input tapes per output tape. The output was packed with 18 bits per data item, resulting in a difficult and expensive program read on any machine except a 36 bit computer. The University of Maryland Computer Science Center has obtained new tape drives capable of writing tapes at 6250 BPI. With this tape density, the output can now be written in a card image form, and still obtain a high packing density, and facilitate the interchange of the output tapes to other computers. To reduce the complexity and the cost involved in reading the TREND tapes by the potential user, the program "REPACK" was developed. About 20 input tapes are converted into one output tape, using this format. The final output produced is seven magnetic tapes having the internal numbers:

P12389; P12870; P12868; P12392

P11898; P12391; P11899

Detailed information about the content of these tapes is given in Pinker and Kaylor, (1983b).

PROCESSING OF THE WIND DIRECTION DATA

During the experiment, wind direction and wind speed were written on two separate tape systms, with no correspondence between start and stop times for the tape files. The direction

values were rewritten at Watervliet ARS onto separate tapes. Two
or three input ('A') tapes were rewritten to one output tape but
not necessarily in the proper sequence. One direction file will
normally contain one or more speed files, but speed files may
overlap two direction files.

Program "Vector" attempts to merge the wind speed and
direction measurements. Wind speed was measured every 10
seconds, while wind direction was measured every 20 to 30
seconds. The vector components are computed at the wind speed
times, on the assumption that the speed is more variable than the
direction. A linear interpolation is performed on two directions
to derive a direction at the time of the wind speed measure-
ment. Directions are digitized to approximately 0.01 radian
increments and a table look-up method used for the sine and
cosine components. A working data set was prepared covering the
months of February, April-May, June, August, 1970. These 30
second wind velocities are stored at the University of Maryland
under the internal tape numbers:

P21481; P22318; P15969; P12871; P19762

Half hourly averages were also obtained and are stored under the
internal tape numbers:

P21482; P21278; P17653

A CONDENSED WORKING DATA SET

From the overwhelming data base at our disposal, a "working"
data set of half hourly averaged data was prepared. These half
hourly averages were obtained for various periods of the monsoon
cycle, for about two weeks each. Since the reduction process is
time consuming and expensive, this useful set of data was stored
on a separate tape. From the half hourly data, two week averages
were obtained. These are also stored on the same tape. This
9-track tape (internal tape Number P10629) contains 170 files,
each of which contains wind speed and temperature data. The tape
is unlabled and contains field data code character representation
with a storage density of 6250 bpi.

A set of all the described tapes is stored at the Department
of Meteorology, University of Maryland, College Park, Maryland
20742. A copy of the repacked "D" tapes and the "merged" (wind
speed and direction) working set, will also be kept at the U.S.
Army Atmospheric Sciences Laboratory, White Sands Missile Range,
New Mexico 88002-5501. Inquiries should be directed to the
attention of Ronald M. Cionco.

END
FILMED

3 -86

DTIC